MV009 - Convex Bowl

An Exploration of Precision

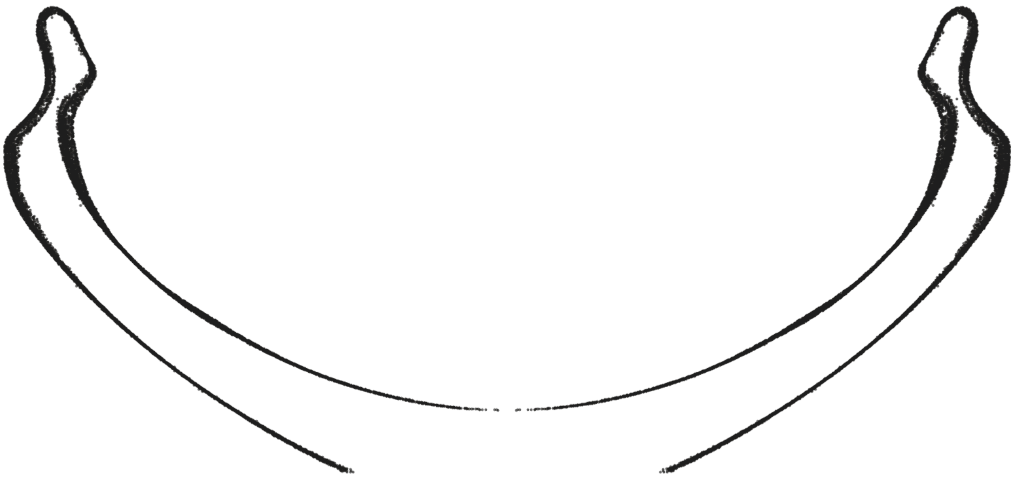

Author: Stine Gerdes, arcsci.org

Date: 2025-03-18
Version: 01.00

Petrie Museum, CC BY-NC-SA

Contents

Artifact Information

Artifact Data

Collection	Petrie Museum of Egyptian Archaeology
Provenance[1]	Petrie Museum of Egyptian Archaeology (London), recovered by Flinders Petrie
Provenience[2]	Unknown
Attribution	3rd Dynasty

Museum information

Ref.	LDUCE-UC17722
Description	Banded grey Diorite gneiss bowl, part of rim missing.
URL	https://collections.ucl.ac.uk/Details/collect/58807

Maijers vessel classification[3]

Short classification	Convex Bowl
Long classification	The vessel is created in an open form classified as a bowl with a convex shape, the vessels Convex curves are ending in a carinated rim.

Physical properties

Precision score[4]	16
Height (approximate)	58 mm 2.28 in
Width (approximate)	123 mm 4.84 in
Material	Diorite
Mohs Hardness[5]	5.5 - 7 (Diorite)
Weight	

Scan information

Source	Scanned by Artifact Foundation
Source file name	UC17722_base_0.09.stl
Scan method	Laser
Scanner	FreeScale Combo+
Rated scan accuracy	37 µm | 1.51 thou
Scan date	2024-10-14
Scanned by	Károly Póka

Mesh decimation	None, raw scan file used in the analysis
Number of vertices	8 015 998
Mesh density[6]	36 µm | 1.41 thou
Max vertex distance	138 µm | 5.443 thou
Min vertex distance	0 µm | 0.000 thou
Vertices per cm2	21 876 (approximated)
Vertices per in2	141 135 (approximated)

[1]The verifiable chain of custody of an artifact

[2]The location or site where an artifact was recovered

[3]Vessel artifact classification developed by W. Arnold Maijer and described in his publication Masters of Stone, ISBN 978-90-829212-0-5

[4]The precision score metric is described in Precision Score Of The Artifact, p. 48

[5]The Mohs scale is an ordinal scale, from 1 to 10, describing the materials resistance to abrasion (the ability of harder material to scratch softer material)

[6]Median distance between vertices

Alignment In The Cartesian Coordinate System

For precise and valid measurements of the vessel's geometry to be possible, the points of the scanned dataset must first and foremost be placed optimally in a Cartesian coordinate system. Several alignment methods and algorithms have been tested on a number of different vessels to determine the best way to achieve optimal alignment.

Any misalignment of the artifact will increase the error of the precision measurements, due to the distortion/wobble effect caused by the misaligned object. To visualize this distortion, we can consider a representation of the three-dimensional point cloud data, folded to a two-dimensional plane. This folded representation is obtained by rotating all scanned points around an assumed center axis to y = 0, x > 0, thus resulting in a two-dimensional profile representation of all scanned vertices in the object.

Figure 1 illustrates this effect on a ideal ellipsoid. In the first image, the ellipsoid is perfectly aligned, resulting in a narrow and precise two-dimensional folded profile. As misalignments are introduced, the two-dimensional profile increases in width, visually showing the distortion, causing the error in the precision measurements to increase. While easy to understand visually, this distortion can also be objectively quantified, and as such used to compare the fitness of different assumed center axes against each other, and further to create an automated and solid process for optimal Cartesian alignment of the scan data.

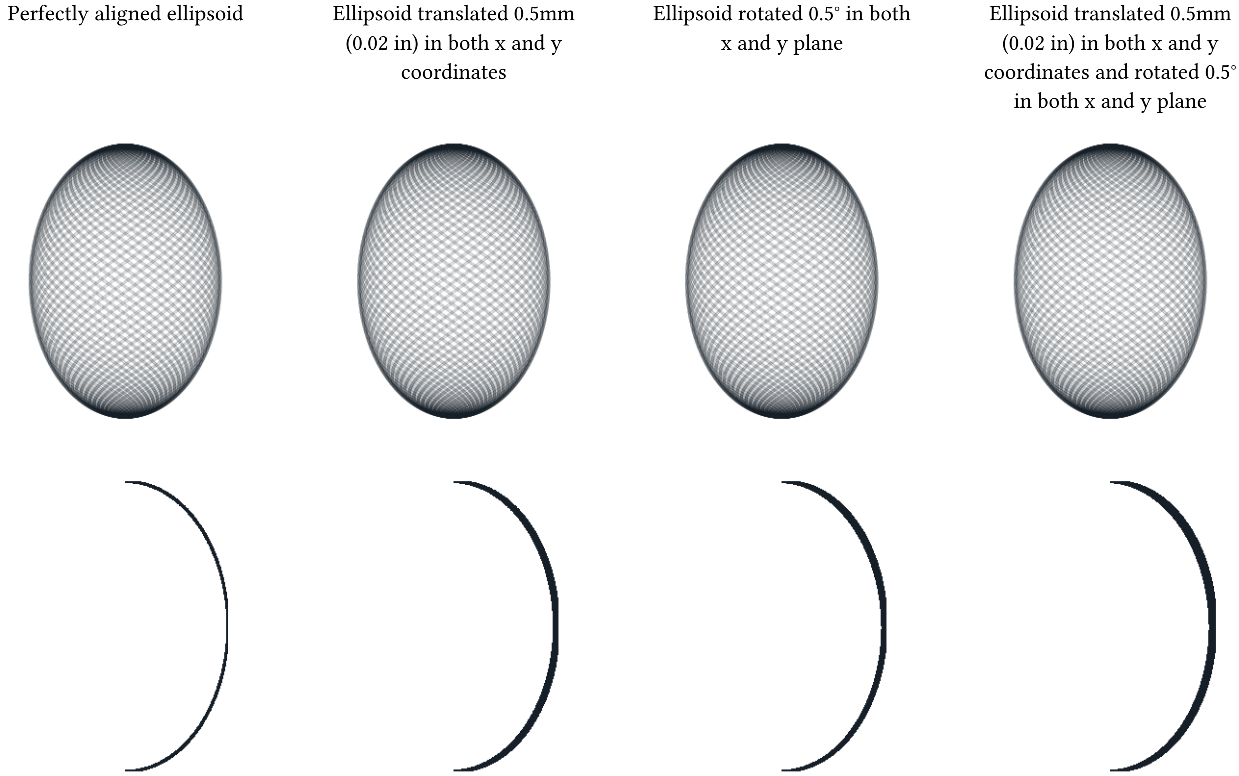

Figure 1: Distortion caused by a misalignment of the artifact

In contemporary metrology analysis of modern production objects, it is common to align the object in a Cartesian coordinate system by fitting a flat surface of the object to a reference plane in the coordinate system, cylindrical features to an ideal cylinder etc., or by using specific markers placed on the object in the design process. This methodology, however, is inadequate for the ancient objects in question. Most scanned artifacts, do not have a valid flat surface which could be aligned to a plane in the Cartesian coordinate system; most surfaces seem to be curved. Some artifacts do have a flat base, however this is often a worn area of the artifact and practical tests have shown that alignment to such surfaces will not produce optimal alignment of the scan data.

As conventional methods of alignment do not always yield good results with these types of artifacts, a more adequate method of alignment has been developed to enable precise measurements and statistical analysis of the scan data.

To find the optimal position of the vessel in the coordinate system, a range of rotation and translation tests are carried out to find the best fit of the central axis.

Based on the assumption that the analyzed object was created using a rotational process, and thus have symmetry around a central axis, the alignment of the artifact is carried out in a two-step process. An overview of this process is given below.

The artifact is placed in a Cartesian coordinate system, in an initially unaligned state. The first step in the alignment process estimates the central rotational axis of the vessel, by analyzing the coaxiality of thin cross-section slices of the vessel. The slices will be as thin as possible based on the mesh density of the scan, while still ensuring enough data points in each slice to be statistically valid.

For each slice, circular regression[7] (estimate of best fit circle) is used to estimate the center point of this slice. Combined over the total Z-axis range of the vessel, these center points provide us with an indicator of the incline and position of the vessel's central axis.

The next step will optimize the center axis alignment by progressively minimizing the deviation (perpendicular to the surface curvature) of the two-dimensional profile, see Figure 1. By ascertaining and comparing the resulting fit of many thousands of different potential rotations, the best fit alignment of the scan data can be estimated, and an optimal center axis (in relation to the data points) can be reconstructed. The actual three-dimensional point-cloud is then aligned to this axis, by rotating and translating the scanned data points to match the Z-axis of the Cartesian coordinate system.

[7]Circle regression algorithm used: Kenichi Kanatani, Prasanna Rangarajan, "Hyper least squares fitting of circles and ellipses" Computational Statistics & Data Analysis, Vol. 55, pages 2197-2208, (2011)

Precision

To explore the manufacturing precision of the artifact in depth, the following analysis have been carried out:

- Circularity around the axis of symmetry is examined in detail at selected cross-sections.
- Overall circularity around the axis of symmetry is measured for the full height of the vessel (areas of the vessel with extensive damage are not taken into account for this metric).
- Concentricity of the vessel between selected cross-sections are examined in detail to determine if the existence of an axis of rotation in the manufacture of the object can be established.
- The coaxiality of the vessel is analyzed to explore the precision of the central axis of the object.
- The surface variability is analyzed and visualized on through a heatmap.

Circularity

Circularity is the measurement of how round the surface of an object is, optionally in reference to a datum axis. The *circularity tolerance* is the radial distance of two circles, each with their centers in the datum axis, and each of them conforming, respectively, to the minimum and maximum deviations of the data-set to a true circle, see Figure 2.

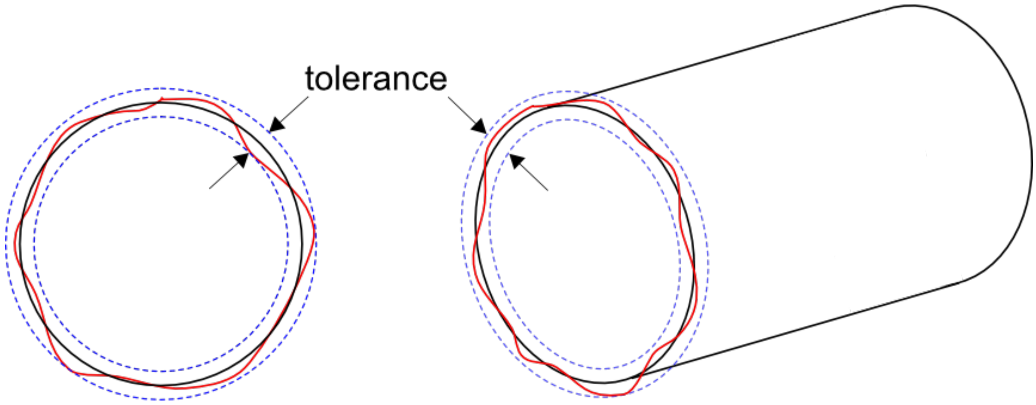

Figure 2: Circularity tolerance.

Circularity is examined at different cross-sections of the vessel, using the established Z-axis as the datum axis (axis of symmetry). The distance between the scanned points in the local datum plane is measured to determine the range between the two concentric circles encompassing the measured points, see Figure 3.

Referencing all of the individual circularity measurements to the global (reconstructed) axis of symmetry of the object, allows us to ascertain not only circularity of local features of the object, but how well circularity was *maintained* over the entire manufacturing process. This is an important distinction, which may be able to provide valuable insights into requirements of the construction methods. For reference, and seeing that the variance in local circularity also holds interest, measurements of circularity of the vessel without reference to the axis of symmetry can additionally be found in the Concentricity, p. 26.

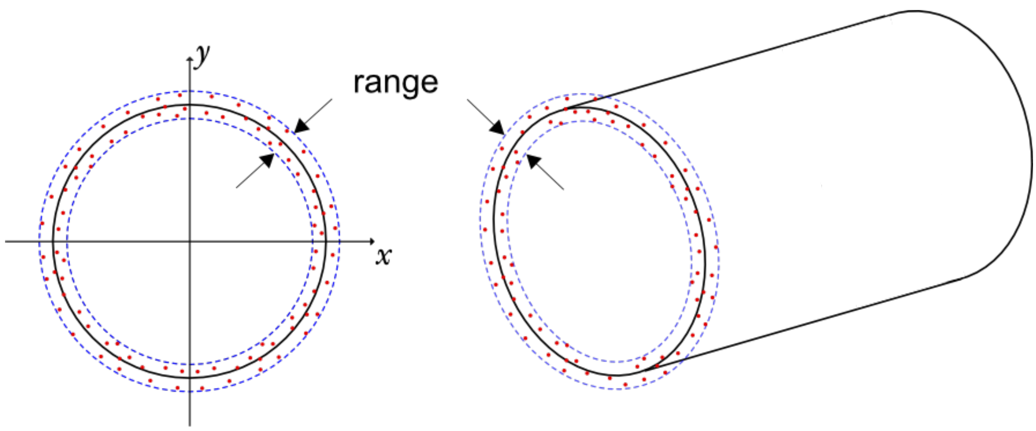

Figure 3: Circularity measurements.

If the circularity is determined from slices of the vessel exclusively in the *Z-plane* (actually measuring the cylindricity of a very thin slices of the vessel, in an attempt to approximate circularity), this would - in some areas - introduce significant distortion (increasing measurement errors) in the samples, due to the curvature of the vessel's surface.

Each sample slice of the vessel is therefore obtained perpendicular to the surface curvature, see Figure 5 to Figure 14. The measurements are taken conservatively without filtration of potential outliers.

To explore the potential distortion caused by obtaining samples in the Z-plane only, please refer to Appendix A, where measurements in the Z-plane and measurements perpendicular to surface curvature are compared side by side.

Detailed circularity measurements of selected points

Circularity measurements across a range of selected slices of the vessel (see Table 1) have been analyzed in-depth, and detailed plots of each measurement is provided. Furthermore, full circularity measurements are shown for each available scanned surface including a detailed plot to visualize the circularity of all areas of the vessel.

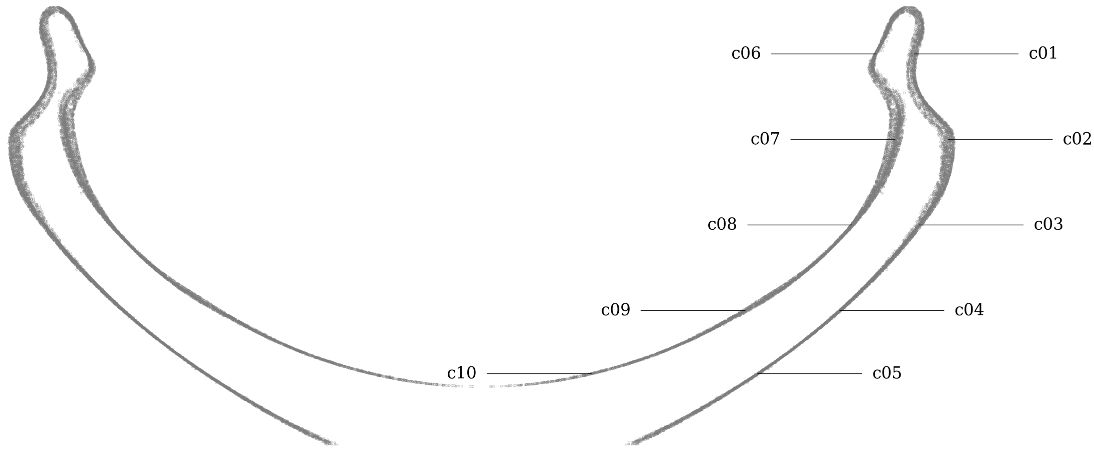

Figure 4: Circularity measurement sample location on MV009.

Metric

Tag	Area	Measured deviation[8]	Residuals				Sample size	Slice		
			Range	RMSD[9]	MAD[10]	SD		Height	Z coord.	Radius[11]
		mm	mm	mm	mm	mm		mm	mm	mm
c01	exterior	Ø113.246±0.701	1.175	0.310	0.268	0.310	2726	0.050	51.298	56.623
c02	exterior	Ø122.202±1.178	1.981	0.492	0.413	0.492	3558	0.050	40.124	61.101
c03	exterior	Ø114.578±0.622	0.924	0.173	0.077	0.173	2725	0.050	28.951	57.289
c04	exterior	Ø93.801±0.362	0.539	0.058	0.043	0.058	1884	0.050	17.777	46.900
c05	exterior	Ø72.286±0.234	0.439	0.048	0.030	0.048	1225	0.050	9.520	36.143
c06	interior	Ø103.201±0.392	0.557	0.081	0.058	0.081	2404	0.050	51.298	51.601
c07	interior	Ø108.287±0.993	1.918	0.478	0.294	0.478	4295	0.050	40.124	54.144
c08	interior	Ø96.987±0.206	0.384	0.093	0.086	0.093	2218	0.050	28.951	48.494
c09	interior	Ø69.036±0.265	0.499	0.123	0.088	0.123	943	0.050	17.777	34.518
c10	interior	Ø28.742±0.120	0.186	0.046	0.034	0.044	203	0.050	9.520	14.371

Imperial

Tag	Area	Measured deviation[8]	Residuals				Sample size	Slice		
			Range	RMSD[9]	MAD[10]	SD		Height	Z coord.	Radius[11]
		in	in	in	in	in		in	in	in
c01	exterior	Ø4.4585±0.0276	0.0463	0.0122	0.0106	0.0122	2726	0.0020	2.0196	2.2293
c02	exterior	Ø4.8111±0.0464	0.0780	0.0194	0.0163	0.0194	3558	0.0020	1.5797	2.4056
c03	exterior	Ø4.5109±0.0245	0.0364	0.0068	0.0030	0.0068	2725	0.0020	1.1398	2.2555
c04	exterior	Ø3.6929±0.0142	0.0212	0.0023	0.0017	0.0023	1884	0.0020	0.6999	1.8465
c05	exterior	Ø2.8459±0.0092	0.0173	0.0019	0.0012	0.0019	1225	0.0020	0.3748	1.4229
c06	interior	Ø4.0630±0.0154	0.0219	0.0032	0.0023	0.0032	2404	0.0020	2.0196	2.0315
c07	interior	Ø4.2633±0.0391	0.0755	0.0188	0.0116	0.0188	4295	0.0020	1.5797	2.1316
c08	interior	Ø3.8184±0.0081	0.0151	0.0037	0.0034	0.0037	2218	0.0020	1.1398	1.9092
c09	interior	Ø2.7180±0.0104	0.0196	0.0048	0.0035	0.0048	943	0.0020	0.6999	1.3590
c10	interior	Ø1.1316±0.0047	0.0073	0.0018	0.0013	0.0017	203	0.0020	0.3748	0.5658

Table 1: Detailed circularity measurements at selected samples of MV009.

Figure 5 to Figure 14 shows a detailed plots of each circularity measurement.

[8]Sample diameter Ø± maximum measured deviation from measured radius
[9]Root mean square deviation (RMSD) also called Root mean square error (RMSE)
[10]Median absolute deviation
[11]Median sample radius from z-axis

Graphical overview of circularity measurement c01

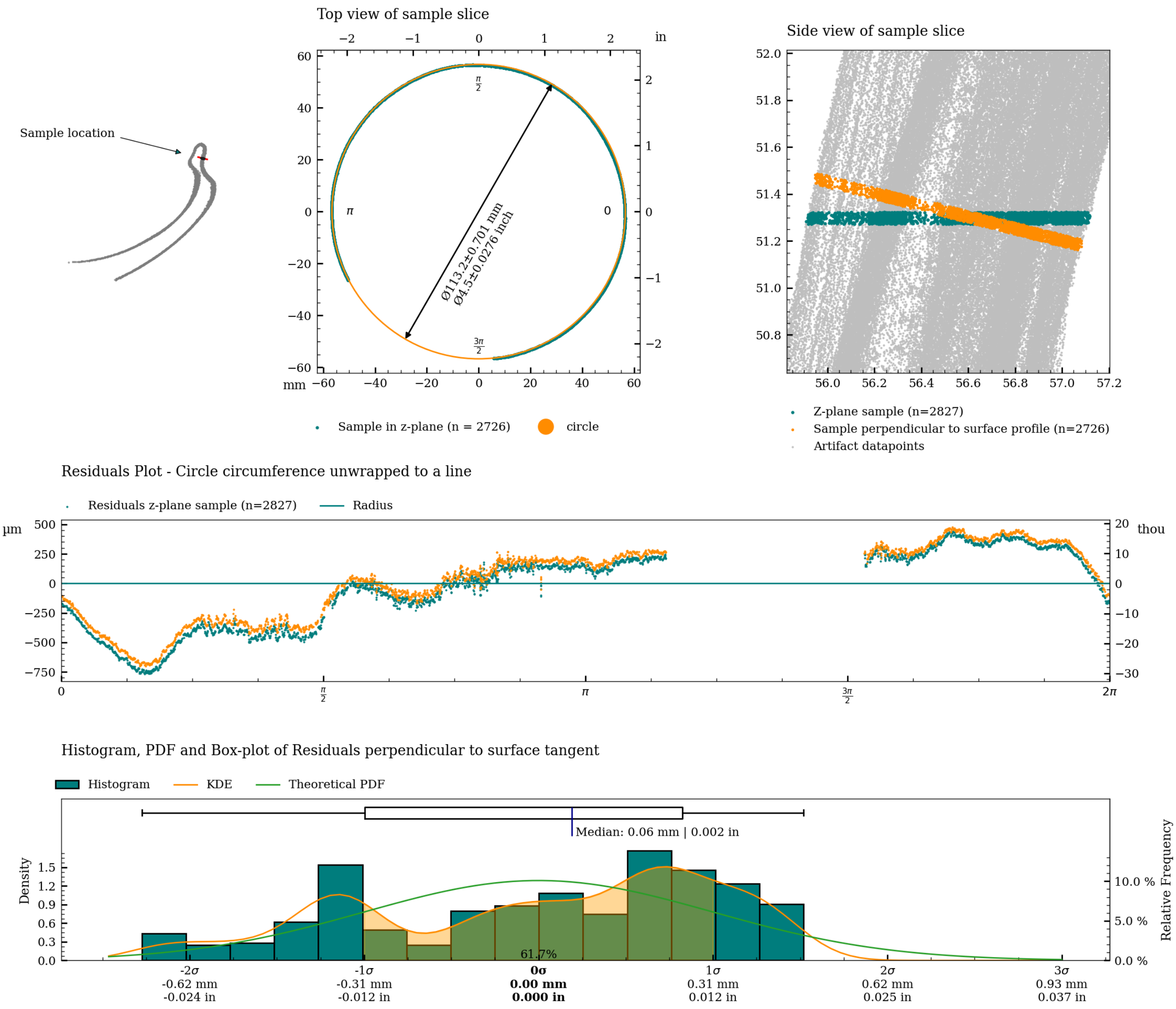

Figure 5: Charts with statistics for the measurement of c01.

Graphical overview of circularity measurement c02

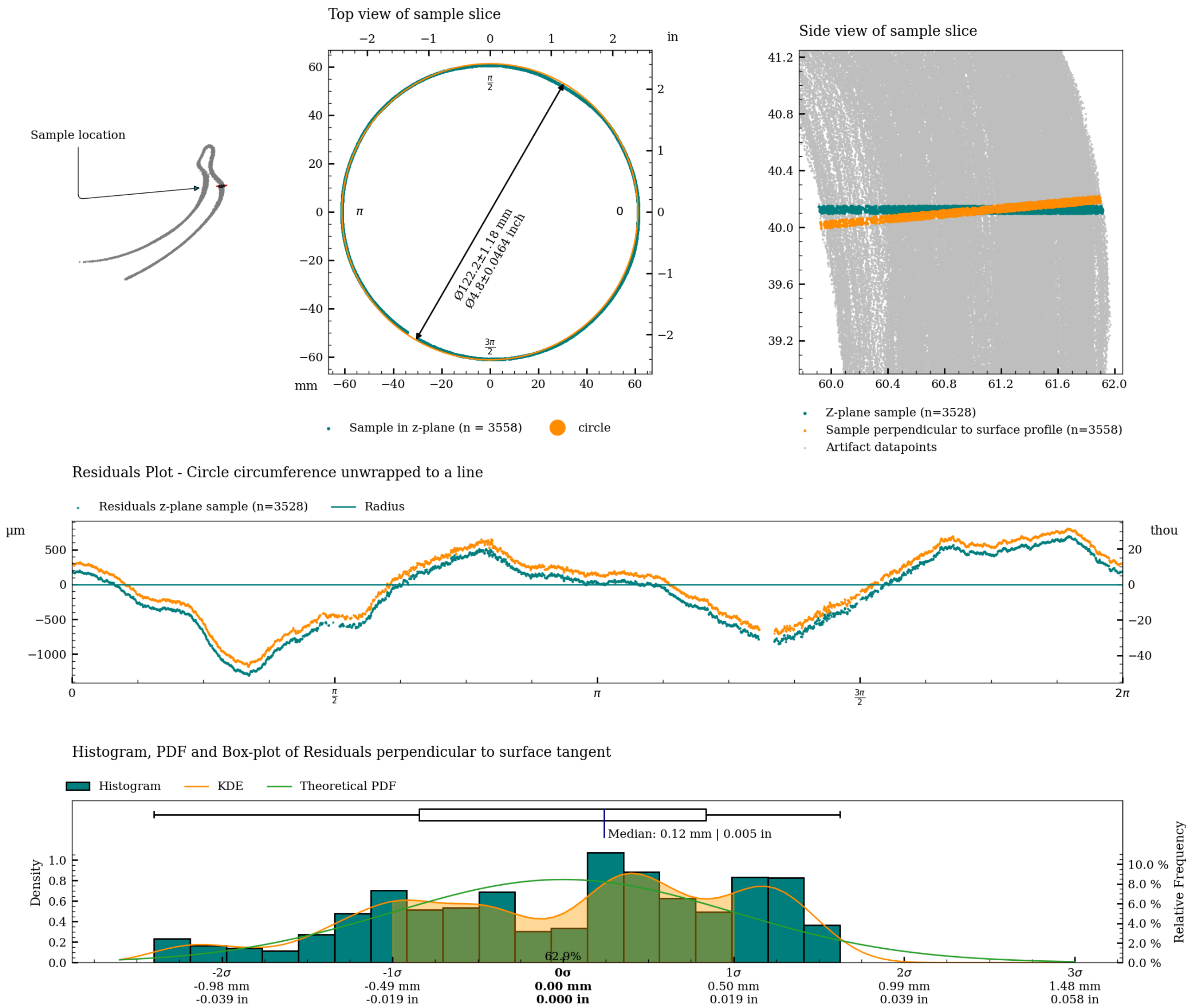

Figure 6: Charts with statistics for the measurement of c02.

Graphical overview of circularity measurement c03

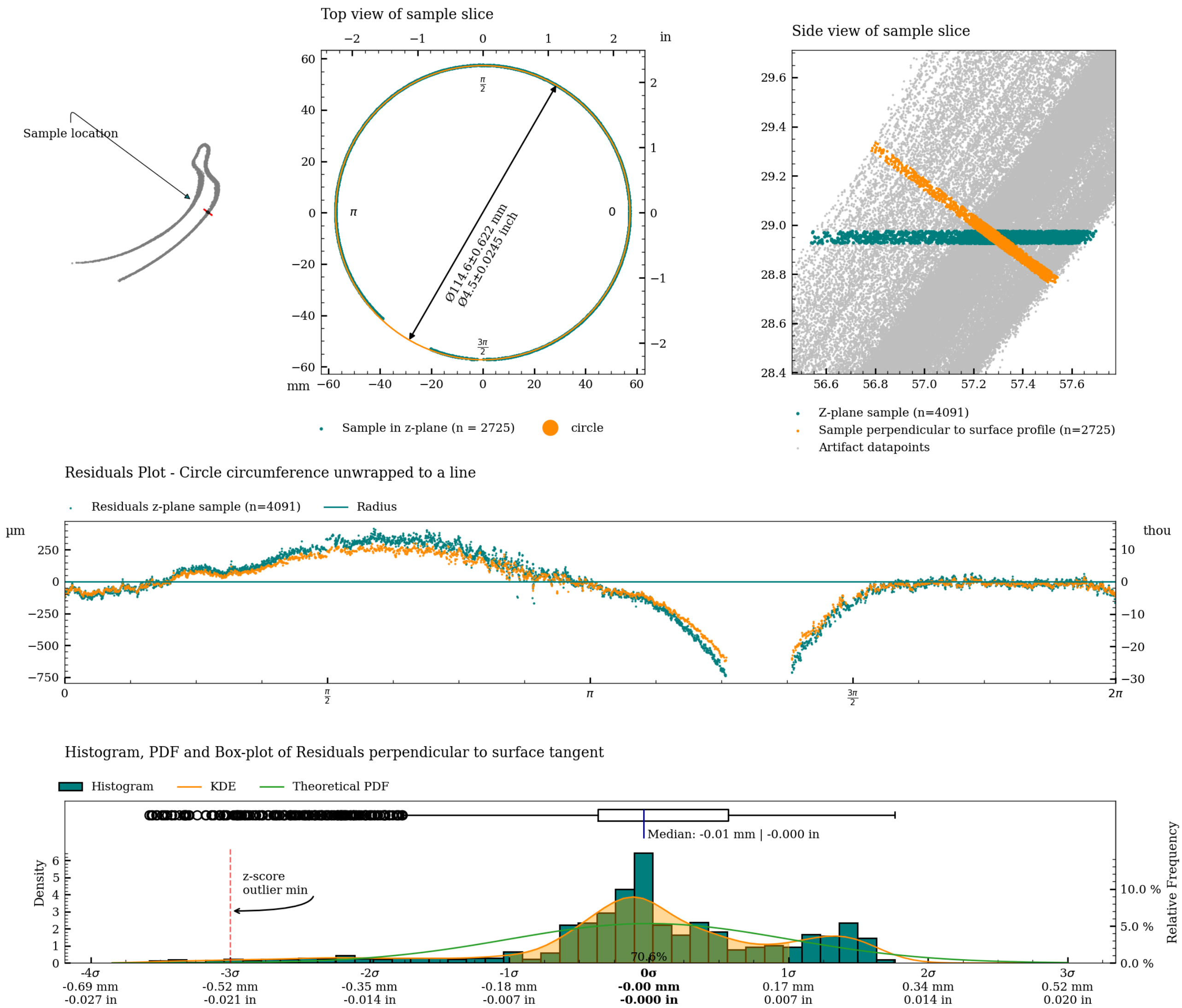

Figure 7: Charts with statistics for the measurement of c03.

Graphical overview of circularity measurement c04

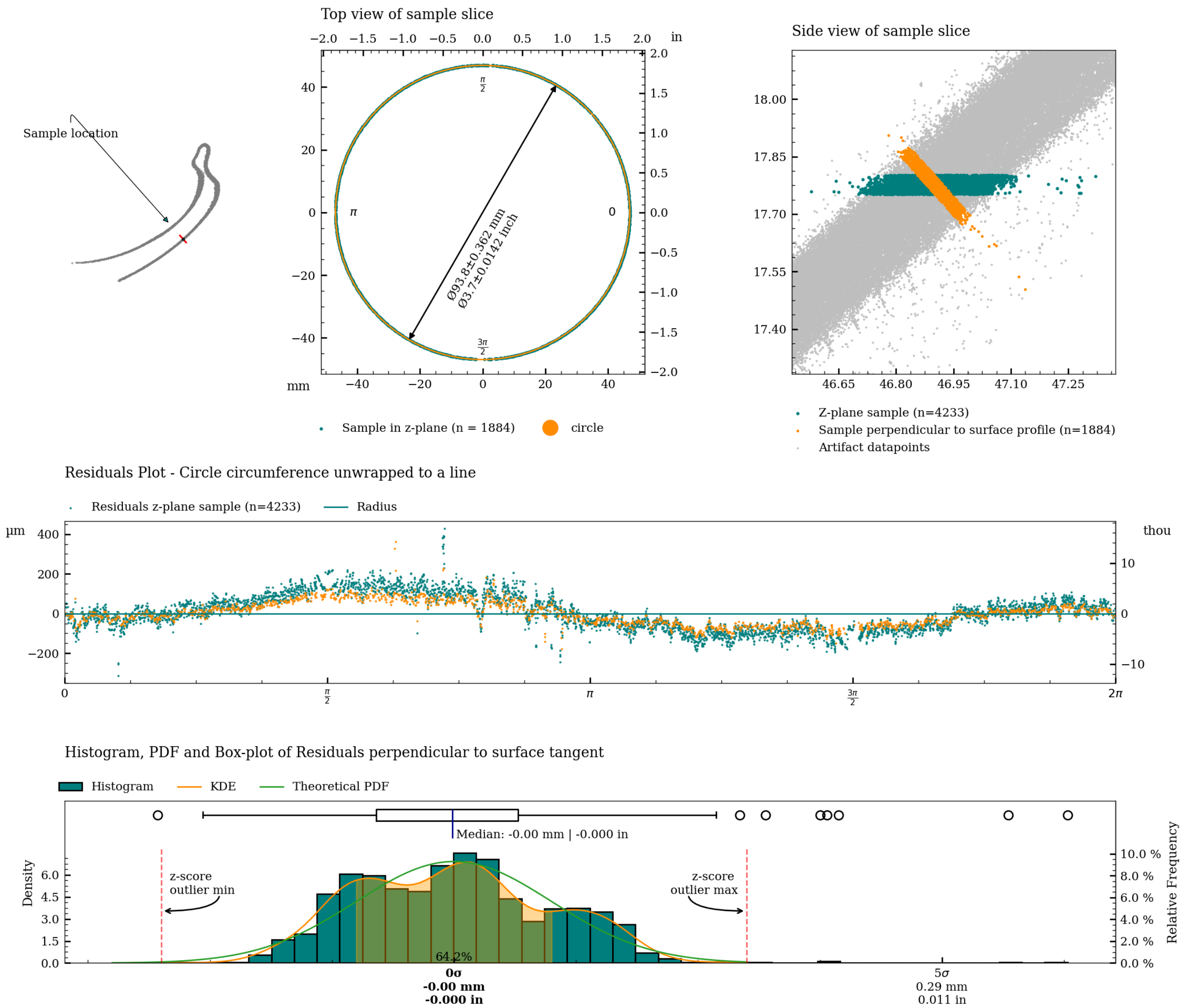

Figure 8: Charts with statistics for the measurement of c04.

Graphical overview of circularity measurement c05

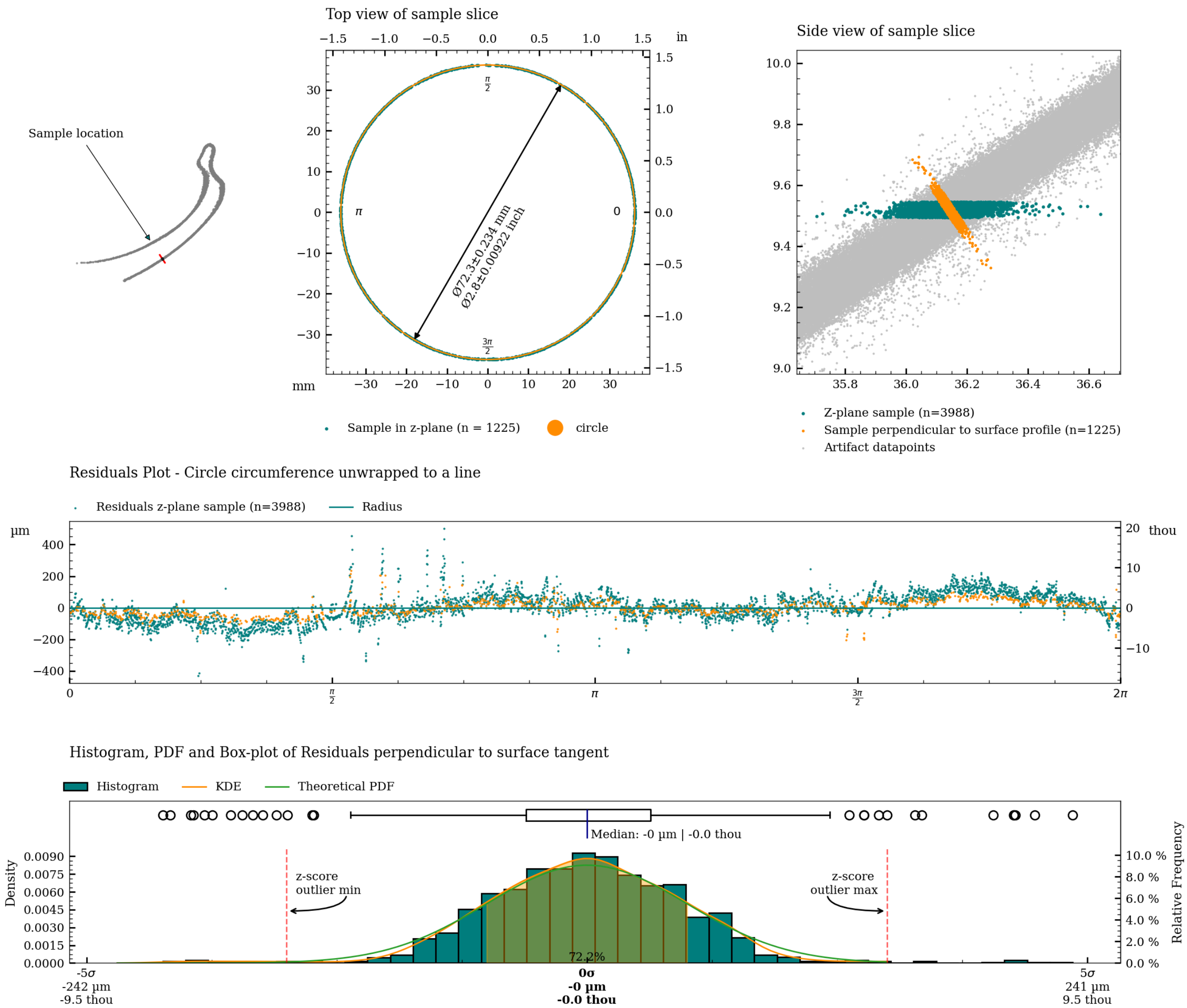

Figure 9: Charts with statistics for the measurement of c05.

Graphical overview of circularity measurement c06

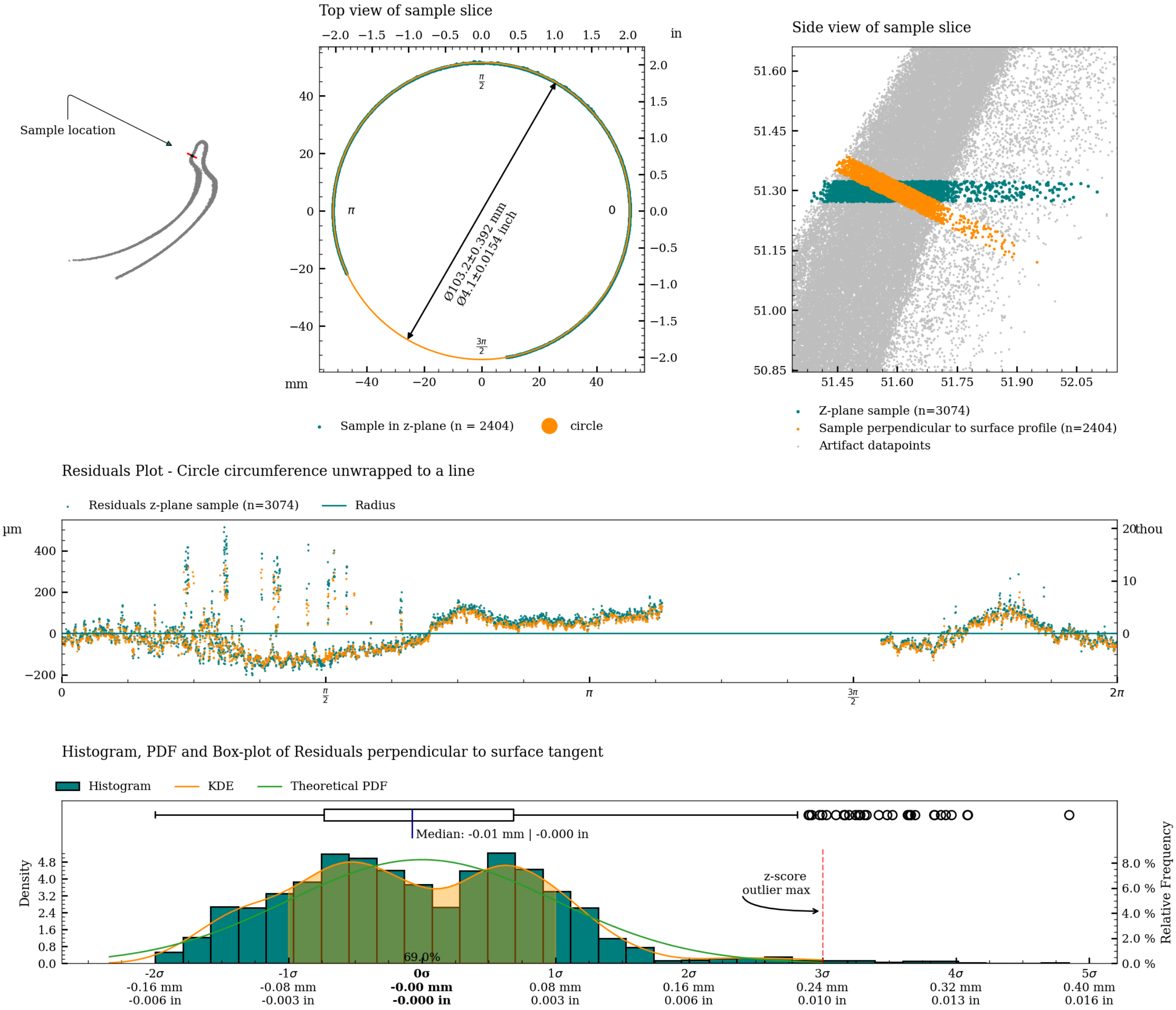

Figure 10: Charts with statistics for the measurement of c06.

Graphical overview of circularity measurement c07

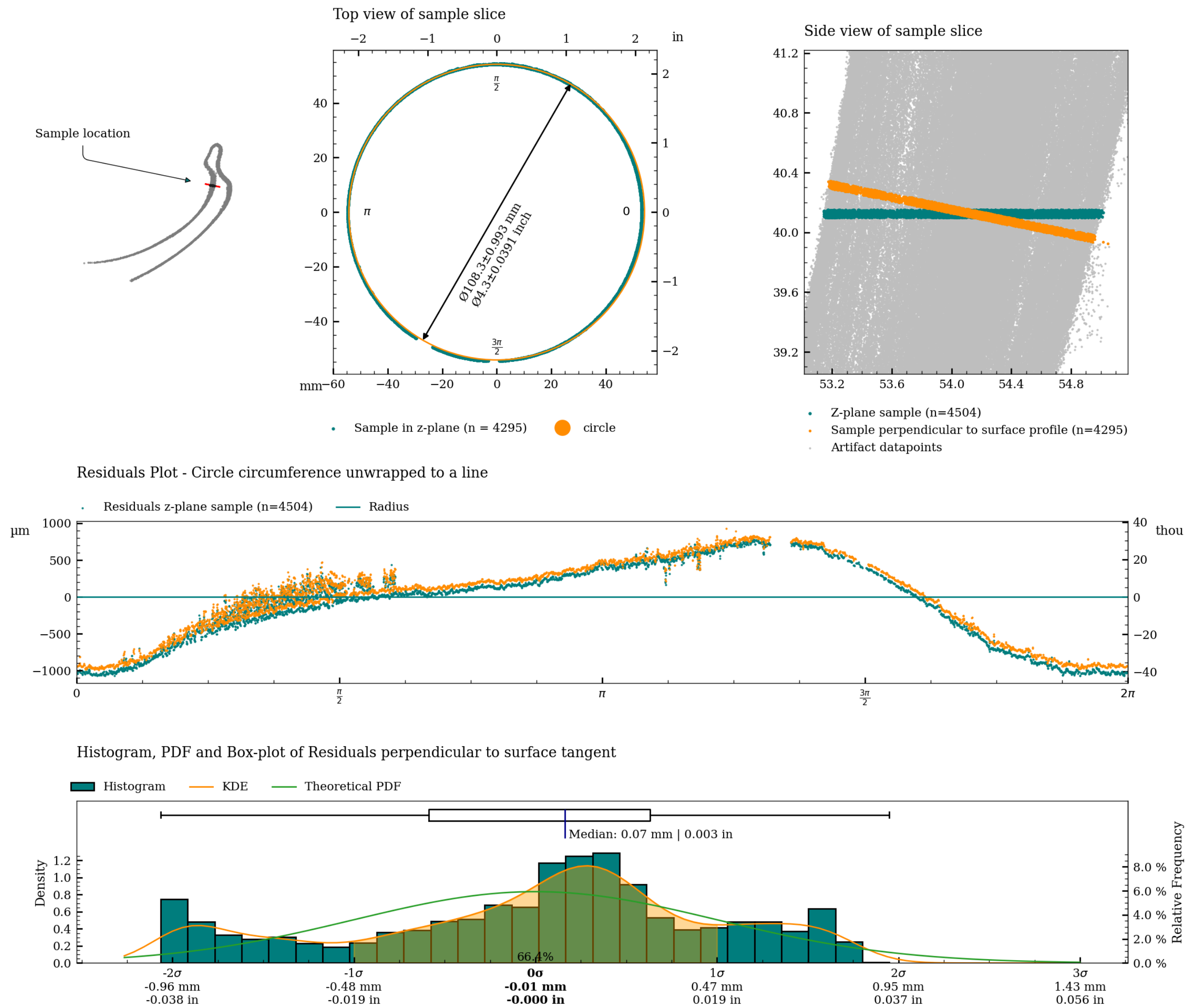

Figure 11: Charts with statistics for the measurement of c07.

Graphical overview of circularity measurement c08

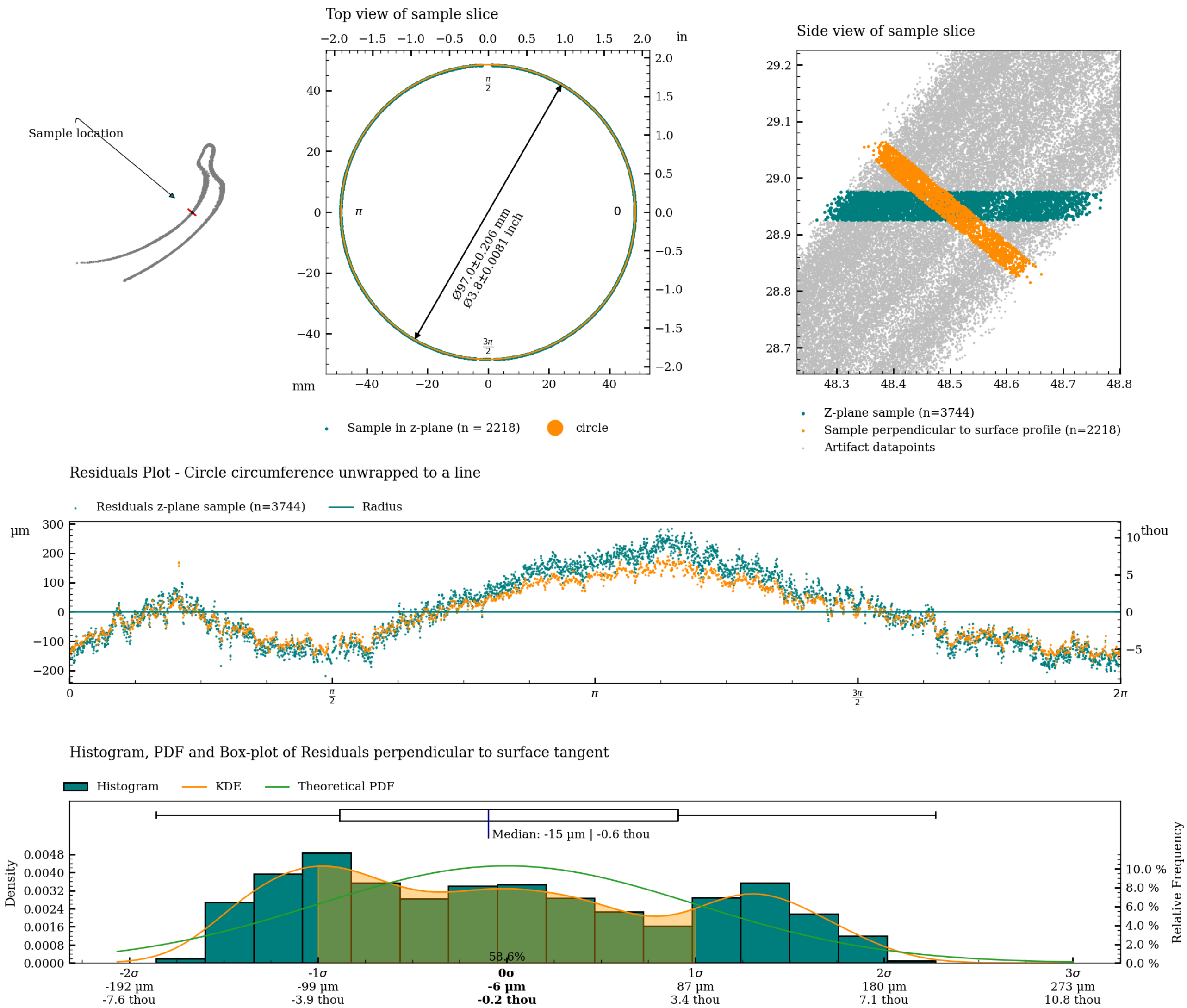

Figure 12: Charts with statistics for the measurement of c08.

Graphical overview of circularity measurement c09

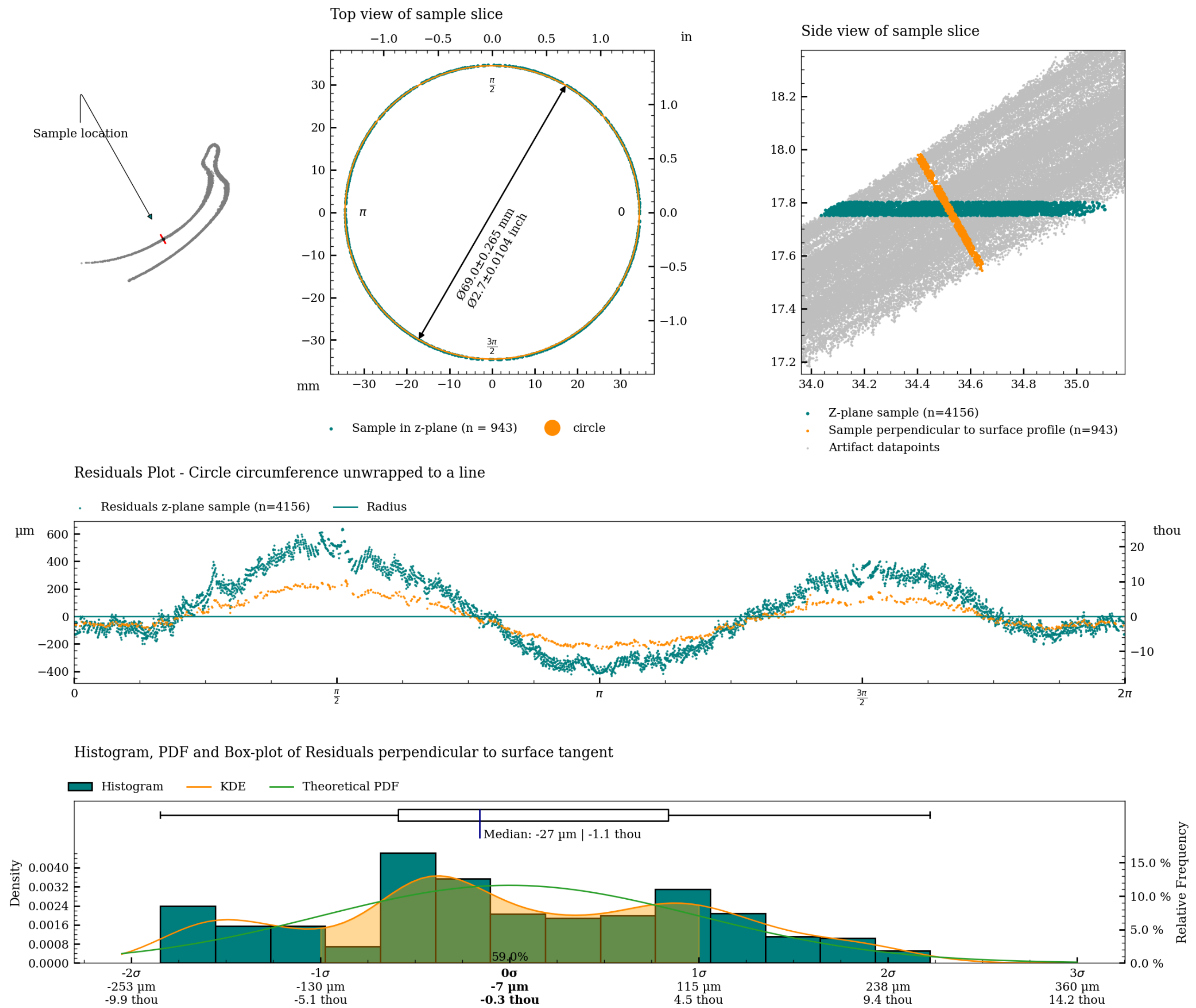

Figure 13: Charts with statistics for the measurement of c09.

Graphical overview of circularity measurement c10

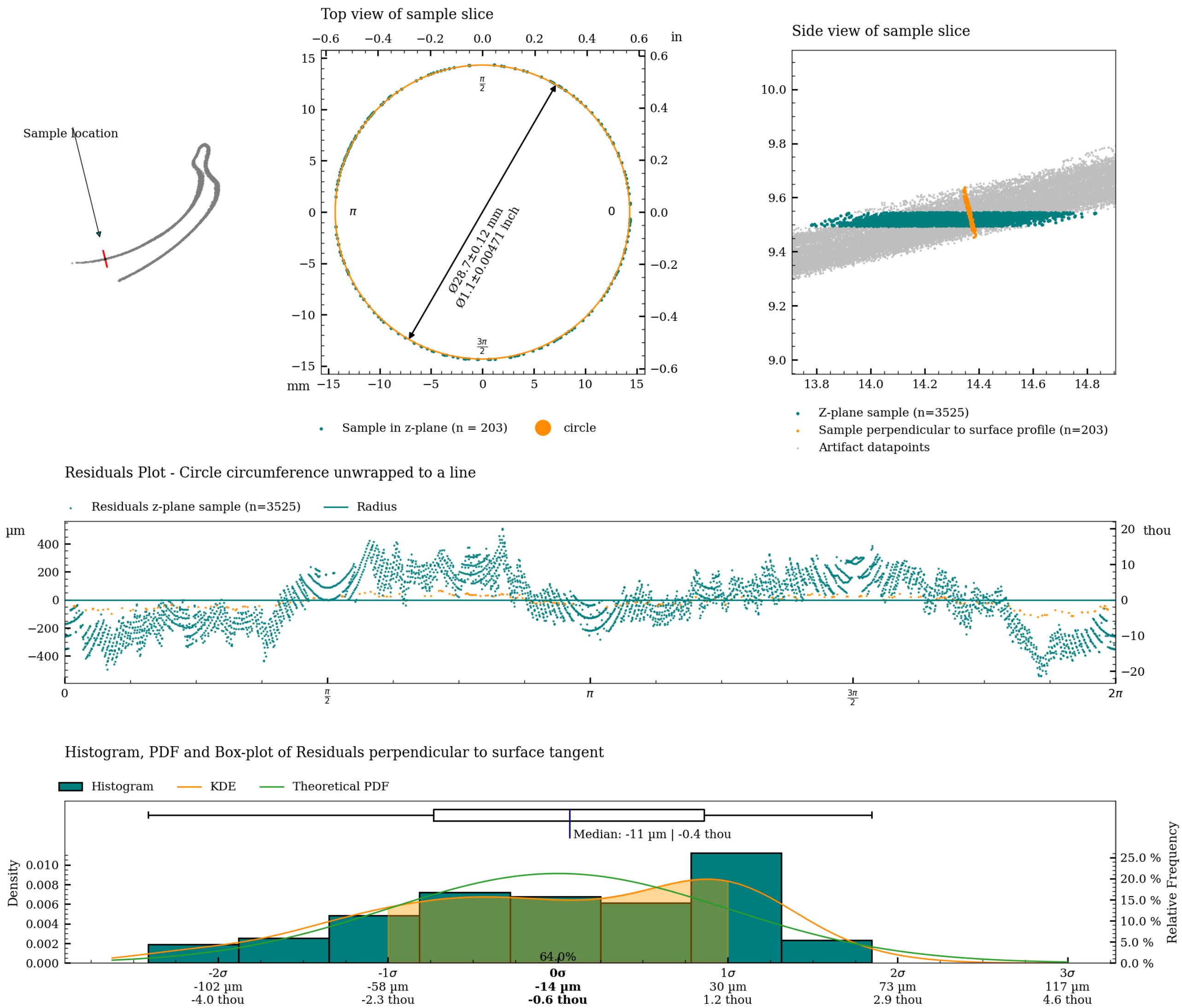

Figure 14: Charts with statistics for the measurement of c10.

Table 2 shows statistical measures of the circularity of the vessel, measured along the full height (damaged parts may reduce the measurement area).

Metric

Area	**Range**			**Standard Deviation**			**Medan Absolute Deviation**			**Slices**	**Slice height**
	Median	**Min.**	**Max.**	**Median**	**Min.**	**Max.**	**Median**	**Min.**	**Max.**		
	mm	mm	mm	mm	mm	mm	mm	mm	mm		mm
Exterior	0.938	0.268	1.989	0.165	0.035	0.499	0.051	0.022	0.426	1133	0.050
Interior	0.665	0.151	2.442	0.141	0.036	0.634	0.058	0.020	0.604	944	0.050

Imperial

Area	**Range**			**Standard Deviation**			**Medan Absolute Deviation**			**Slices**	**Slice height**
	Median	**Min.**	**Max.**	**Median**	**Min.**	**Max.**	**Median**	**Min.**	**Max.**		
	in	in	in	in	in	in	in	in	in		in
Exterior	0.938	0.268	1.989	0.165	0.035	0.499	0.051	0.022	0.426	1133	0.050
Interior	0.665	0.151	2.442	0.141	0.036	0.634	0.058	0.020	0.604	944	0.050

Table 2: Perpendicular Circularity analysis of MV009.

Circularity analysis of exterior surface

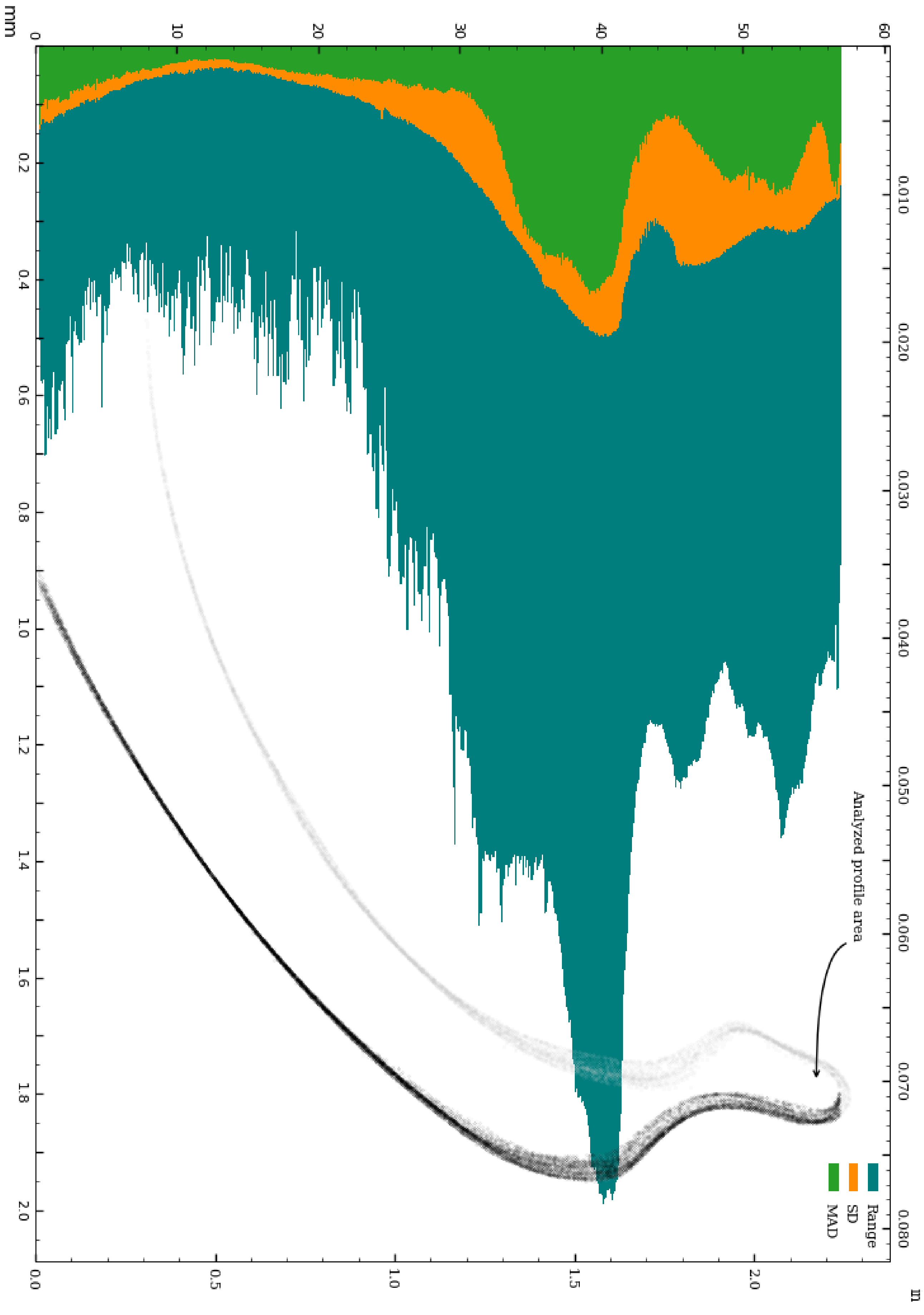

Figure 15: Circularity of exterior surface.

Circularity analysis of exterior surface, Standard Deviation and Median Absolute Deviation

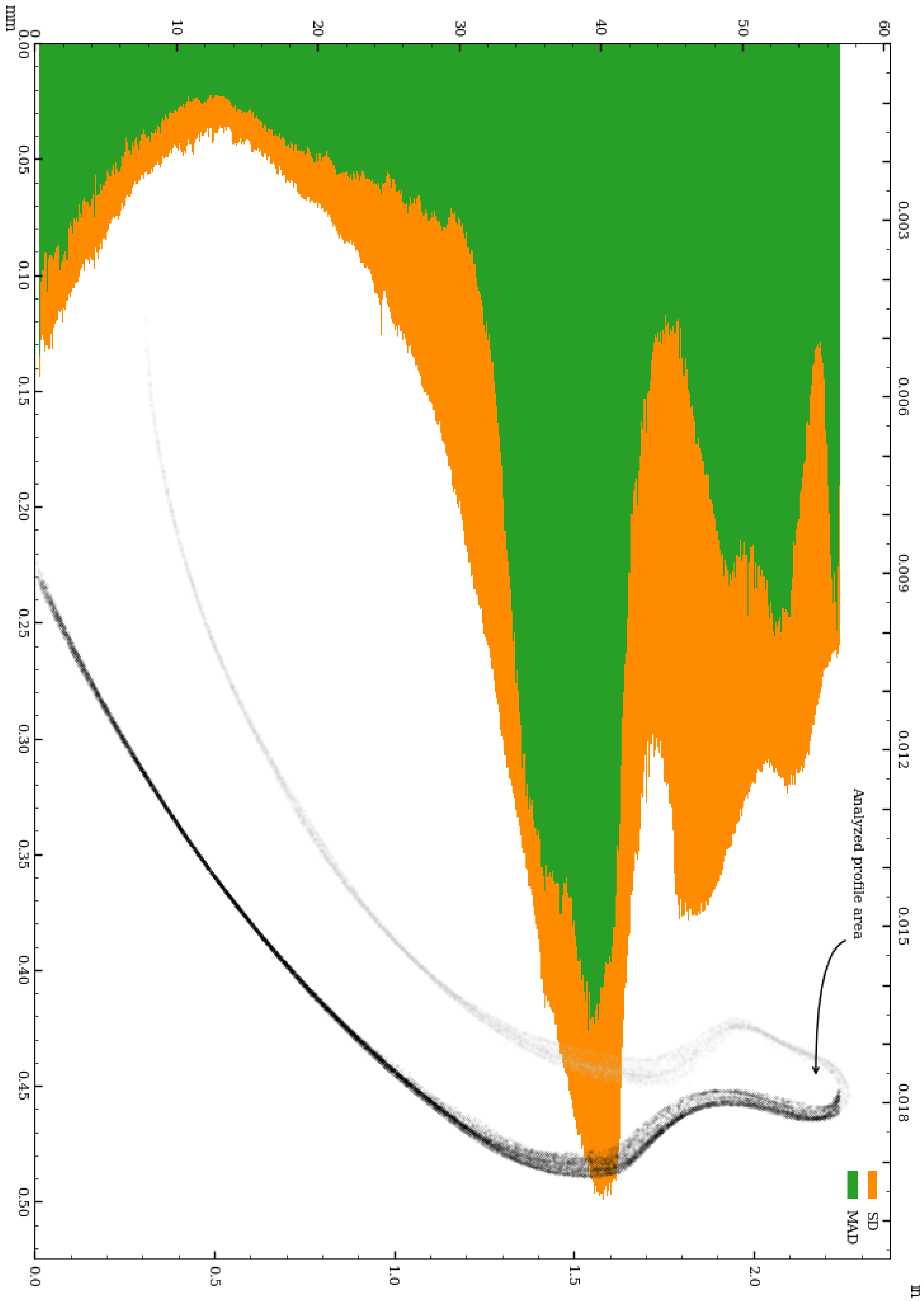

Figure 16: Vessel circularity of exterior surface, standard deviation and median absolute deviation.

The distributions of the circularity measurements across 1133 slices of the exterior surface are shown below.

Range measurement distribution across 1133 slices of exterior surface

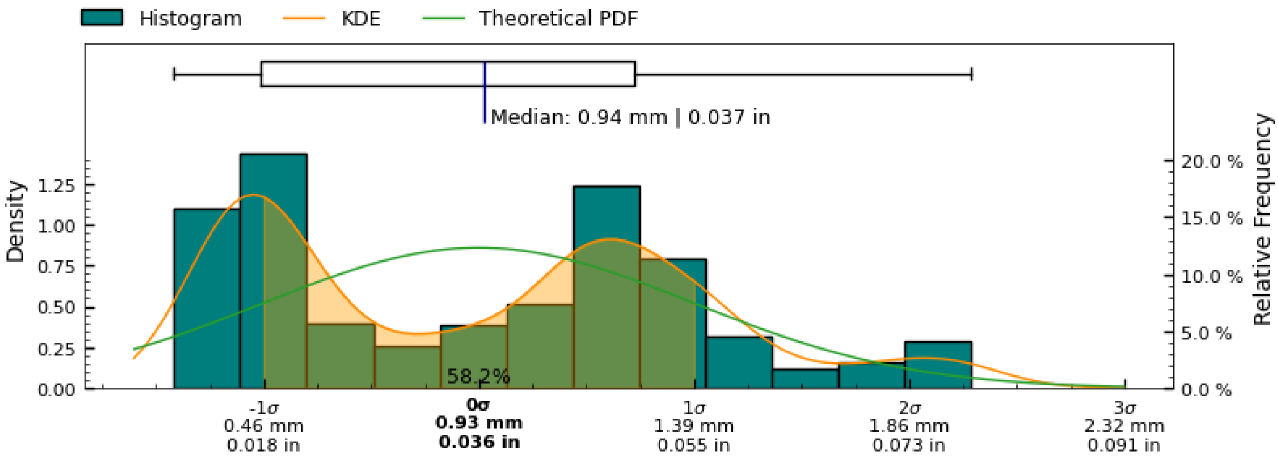

Figure 17: Range measurement distribution across measured slices of exterior surface

Standard deviation measurement distribution across 1133 slices of exterior surface

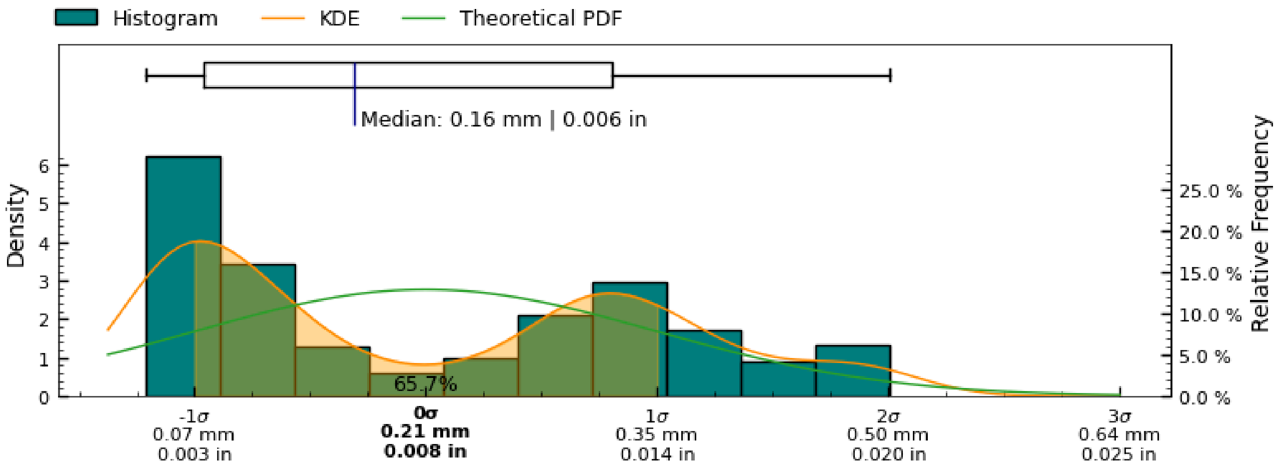

Figure 18: Standard deviation measurement distribution across measured slices of " + exterior + " surface

Median absolute deviation measurement distribution across 1133 slices of exterior surface

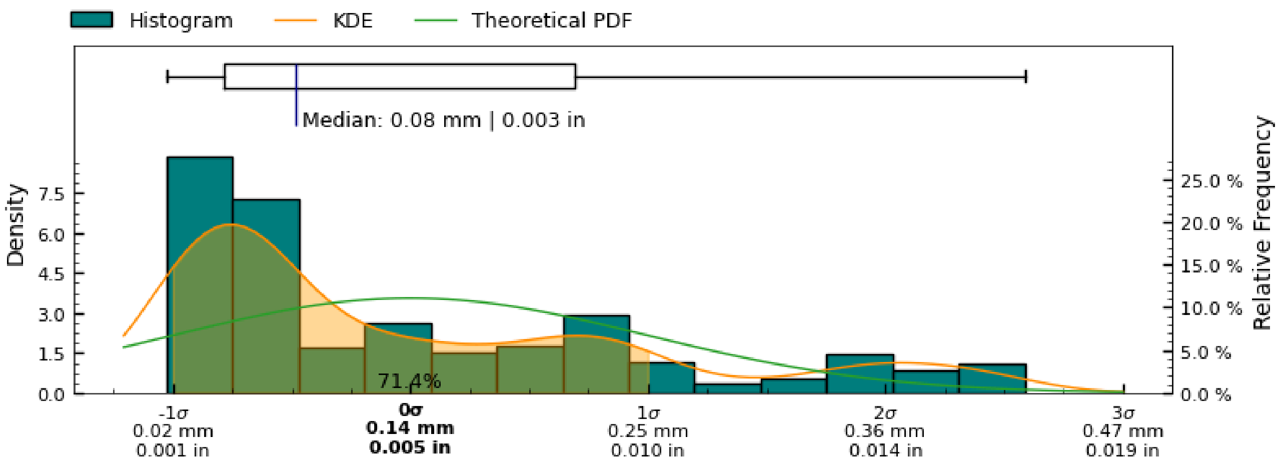

Figure 19: Median absolute deviation measurement distribution across measured slices of exterior surface

Circularity analysis of interior surface

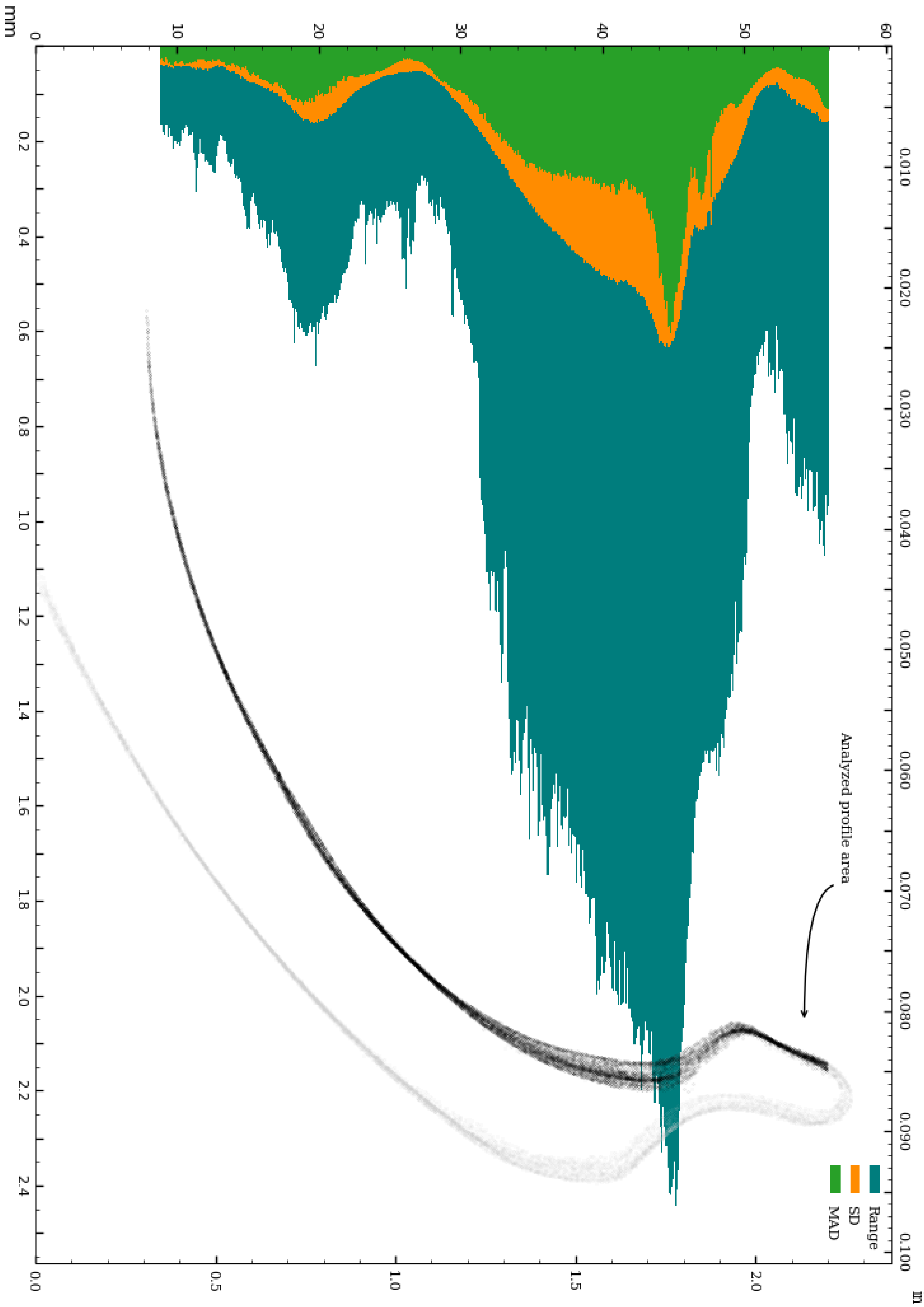

Figure 20: Circularity of interior surface.

Circularity analysis of interior surface, Standard Deviation and Median Absolute Deviation

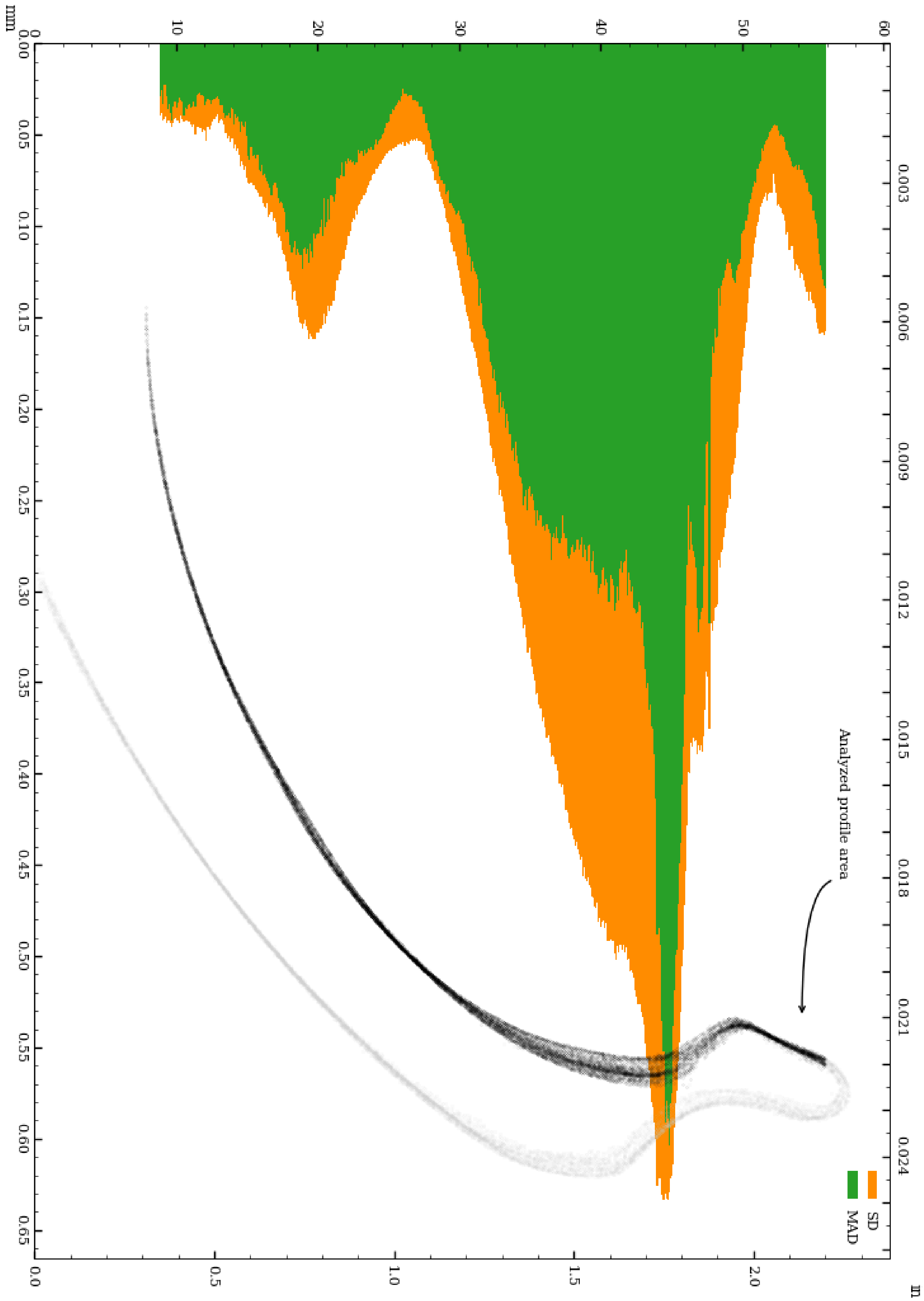

Figure 21: Vessel circularity of interior surface, standard deviation and median absolute deviation.

The distributions of the circularity measurements across 944 slices of the interior surface are shown below.

Range measurement distribution across 944 slices of interior surface

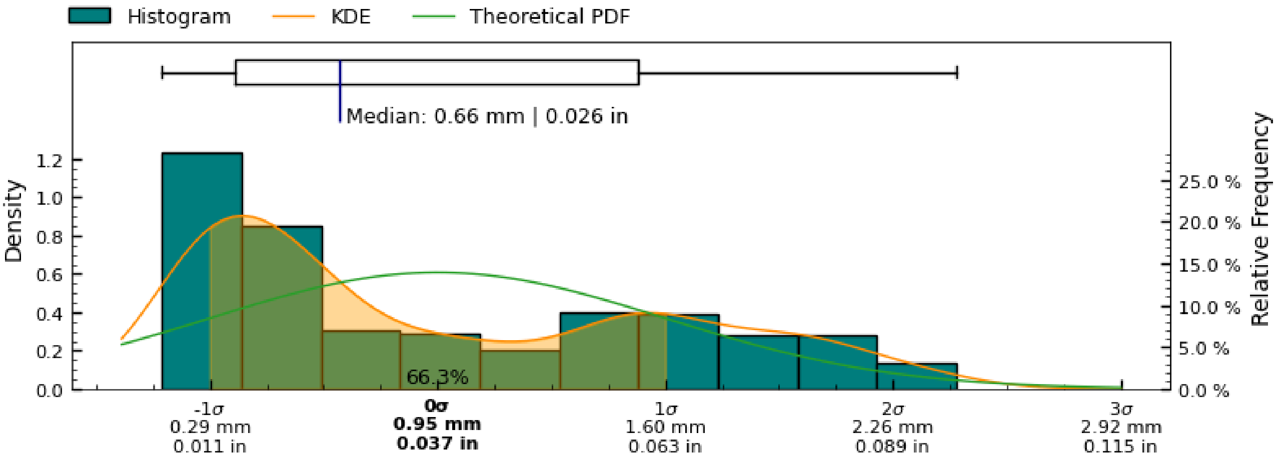

Figure 22: Range measurement distribution across measured slices of interior surface

Standard deviation measurement distribution across 944 slices of interior surface

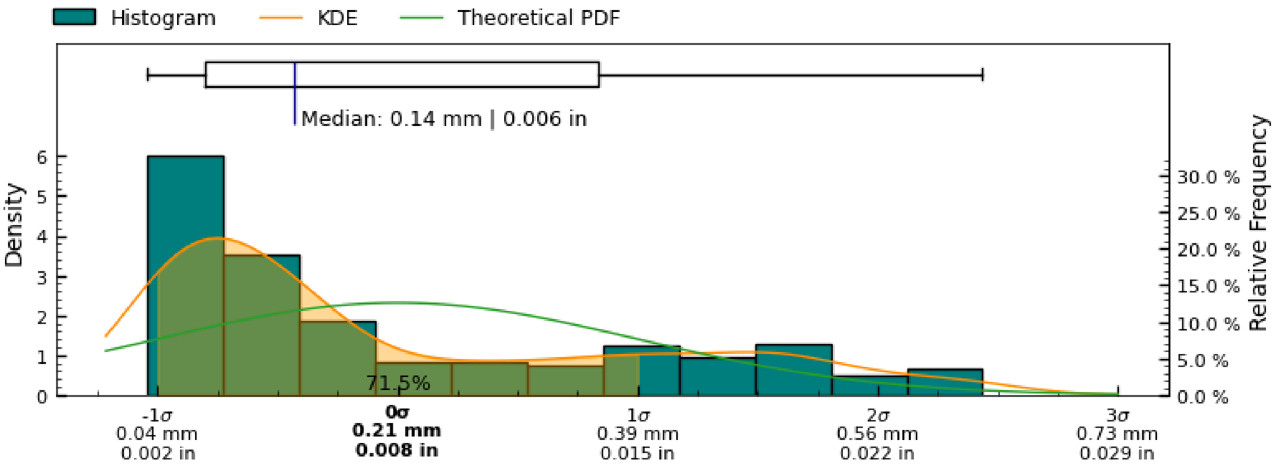

Figure 23: Standard deviation measurement distribution across measured slices of " + interior + " surface

Median absolute deviation measurement distribution across 944 slices of interior surface

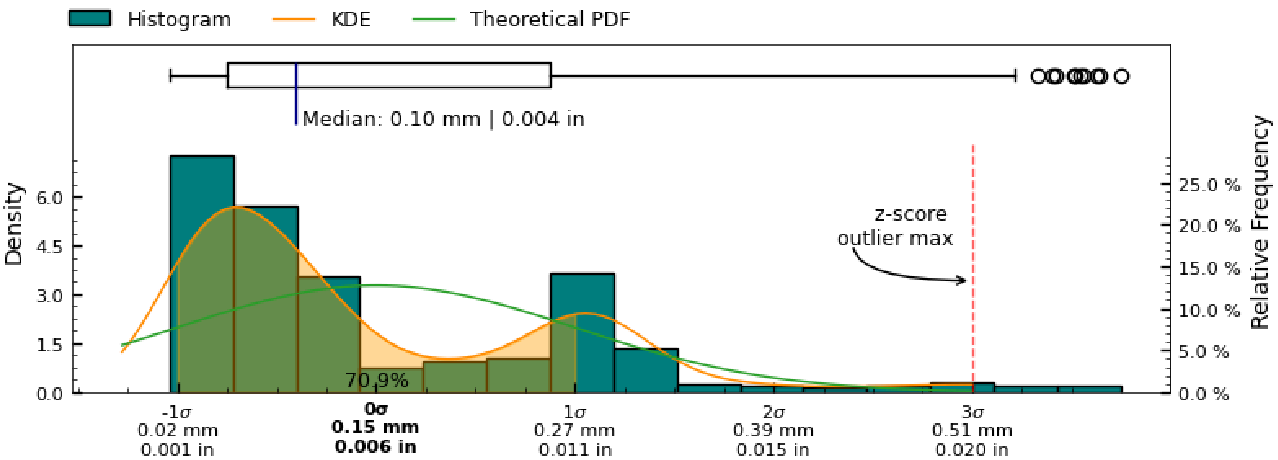

Figure 24: Median absolute deviation measurement distribution across measured slices of interior surface

Concentricity

The concentricity metric describes the deviation in the center-point of the referenced features. As such, it is a measure to determine if several features of the object share the same center point/axis, and how closely. See Figure 25 for a visual representation of this metric.

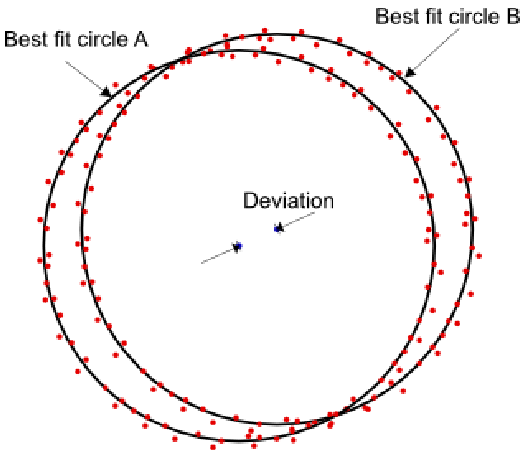

Figure 25: Concentricity measures the deviation (distance) between the center of two circles.

Determination of concentricity has been carried out by establishing the best fit circles of sample slices, using RANSAC (Random sample consensus) algorithm for outlier detection of a least squares circle regression on the scanned data-points at each cross-section, to estimate centers of each cross-section.

The concentricity between both the interior and exterior circular cross-sections is explored for cross-section measurements with the same Z-coordinates.

Additionally, the concentricity between each cross-section measurement defined in Figure 4 and the datum axis $(x, y) = (0, 0)$ has been calculated to establish the deviation of the feature center from the datum axis.

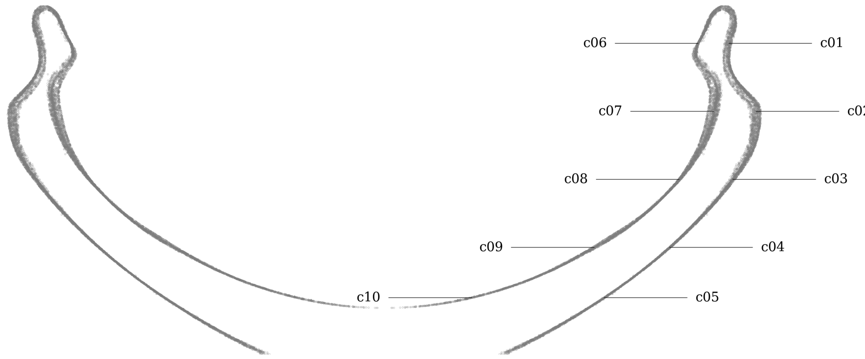

Figure 26: Concentricity measurement sample location on MV009.

Metric

Tag	Reference	Deviation	Sample size	Circle fit residuals analysis for sample listed in Tag column						
				Range full	**Range inliers**	**SD full**	**SD inliers**	**MAD full**	**MAD inliers**	**Center (x,y)**
		mm		mm	mm	mm	mm	mm	mm	µm
c01	z-axis	0.411	2726	1.175	1.175	0.310	0.310	0.218	0.218	−180, −369
c02	z-axis	0.186	3558	1.981	1.981	0.492	0.492	0.404	0.404	39, −182
c03	z-axis	0.141	2725	0.924	0.816	0.173	0.156	0.079	0.076	8, 141
c04	z-axis	0.042	1884	0.539	0.278	0.058	0.055	0.043	0.042	6, 41
c05	z-axis	0.016	1225	0.439	0.236	0.048	0.041	0.030	0.029	−3, −15
c06	z-axis	0.060	2404	0.557	0.313	0.081	0.070	0.058	0.057	−38, −47
c07	z-axis	0.622	4295	1.918	1.918	0.478	0.478	0.286	0.286	−620, −39
c08	z-axis	0.085	2218	0.384	0.384	0.093	0.093	0.078	0.078	−81, −27
c09	z-axis	0.032	943	0.499	0.499	0.123	0.123	0.102	0.102	27, 17
c10	z-axis	0.009	203	0.186	0.186	0.044	0.044	0.035	0.035	−9, −0
c01	c06	0.352	2726	1.175	1.175	0.310	0.310	0.218	0.218	−143, −322
c02	c07	0.675	3558	1.981	1.981	0.492	0.492	0.404	0.404	659, −143
c03	c08	0.190	2725	0.924	0.816	0.173	0.156	0.079	0.076	89, 168
c04	c09	0.033	1884	0.539	0.278	0.058	0.055	0.043	0.042	−21, 25
c05	c10	0.016	1225	0.439	0.236	0.048	0.041	0.030	0.029	6, −15

Imperial

Tag	Reference	Deviation	Sample size	Circle fit residuals analysis for sample listed in Tag column						
				Range full	**Range inliers**	**SD full**	**SD inliers**	**MAD full**	**MAD inliers**	**Center (x,y)**
		in		in	in	in	in	in	in	thou
c01	z-axis	0.0162	2726	0.0463	0.0463	0.0122	0.0122	0.0086	0.0086	−7.1, −14.5
c02	z-axis	0.0073	3558	0.0780	0.0780	0.0194	0.0194	0.0159	0.0159	1.5, −7.2
c03	z-axis	0.0056	2725	0.0364	0.0321	0.0068	0.0061	0.0031	0.0030	0.3, 5.6
c04	z-axis	0.0016	1884	0.0212	0.0110	0.0023	0.0022	0.0017	0.0017	0.2, 1.6
c05	z-axis	0.0006	1225	0.0173	0.0093	0.0019	0.0016	0.0012	0.0012	−0.1, −0.6
c06	z-axis	0.0024	2404	0.0219	0.0123	0.0032	0.0028	0.0023	0.0022	−1.5, −1.8
c07	z-axis	0.0245	4295	0.0755	0.0755	0.0188	0.0188	0.0112	0.0112	−24.4, −1.5
c08	z-axis	0.0034	2218	0.0151	0.0151	0.0037	0.0037	0.0031	0.0031	−3.2, −1.0
c09	z-axis	0.0013	943	0.0196	0.0196	0.0048	0.0048	0.0040	0.0040	1.1, 0.7
c10	z-axis	0.0004	203	0.0073	0.0073	0.0017	0.0017	0.0014	0.0014	−0.4, −0.0
c01	c06	0.0139	2726	0.0463	0.0463	0.0122	0.0122	0.0086	0.0086	−5.6, −12.7
c02	c07	0.0266	3558	0.0780	0.0780	0.0194	0.0194	0.0159	0.0159	26.0, −5.6
c03	c08	0.0075	2725	0.0364	0.0321	0.0068	0.0061	0.0031	0.0030	3.5, 6.6
c04	c09	0.0013	1884	0.0212	0.0110	0.0023	0.0022	0.0017	0.0017	−0.8, 1.0
c05	c10	0.0006	1225	0.0173	0.0093	0.0019	0.0016	0.0012	0.0012	0.2, −0.6

Table 3: Concentricity analysis of MV009.

Concentricity analysis of c01

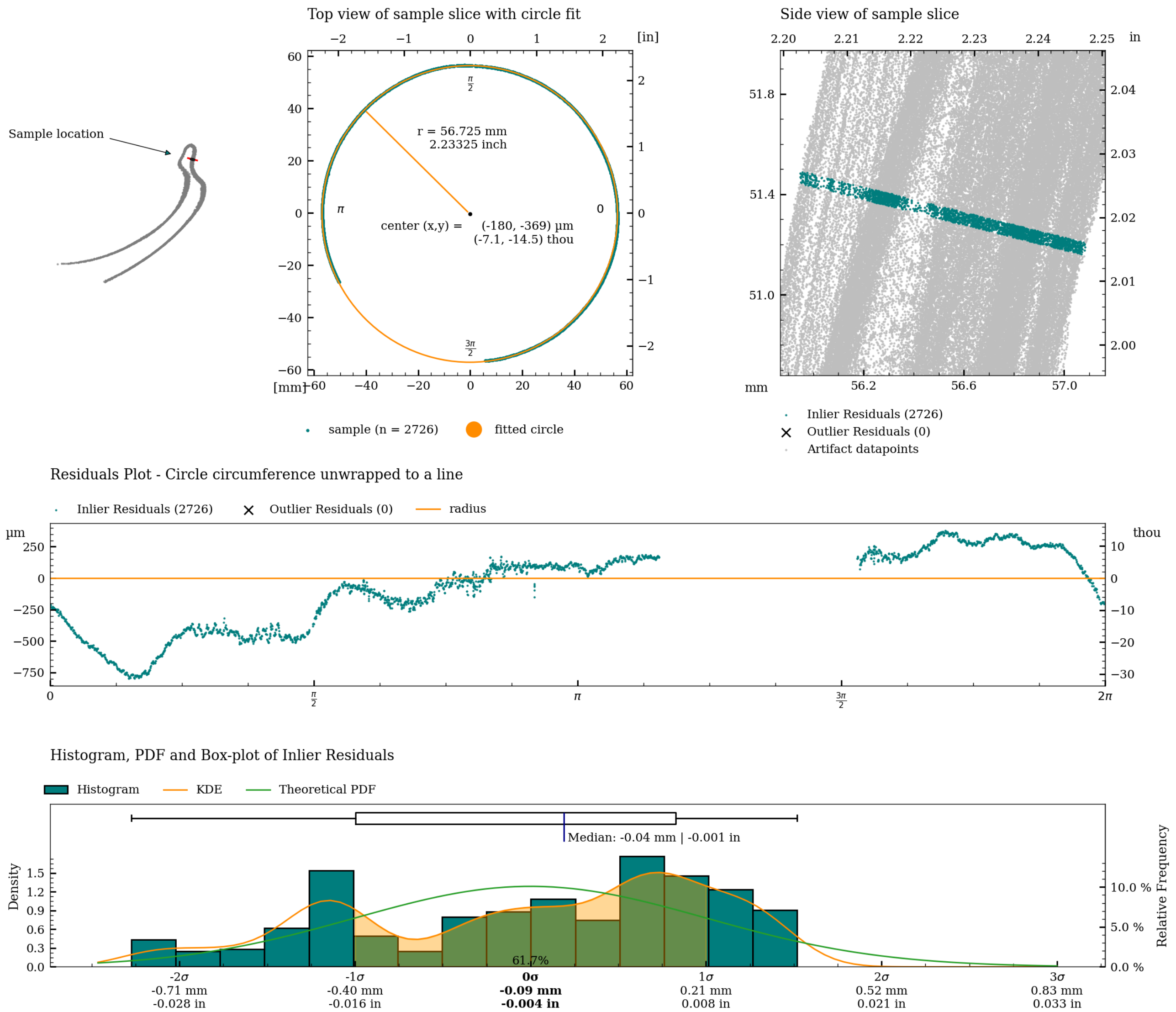

Figure 27: Detailed plot of concentricity measurement for c01.

Concentricity analysis of c02

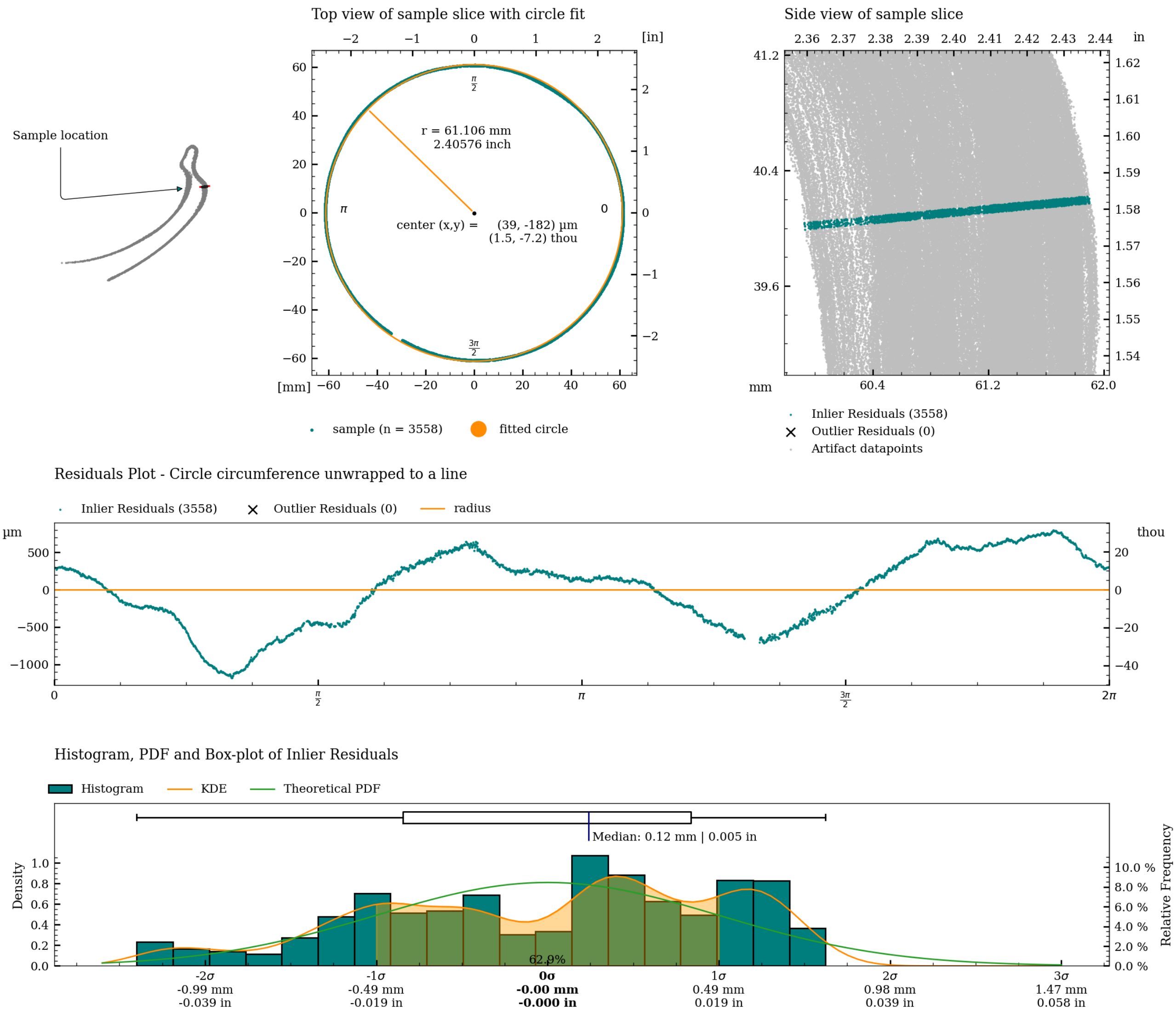

Figure 28: Detailed plot of concentricity measurement for c02.

Concentricity analysis of c03

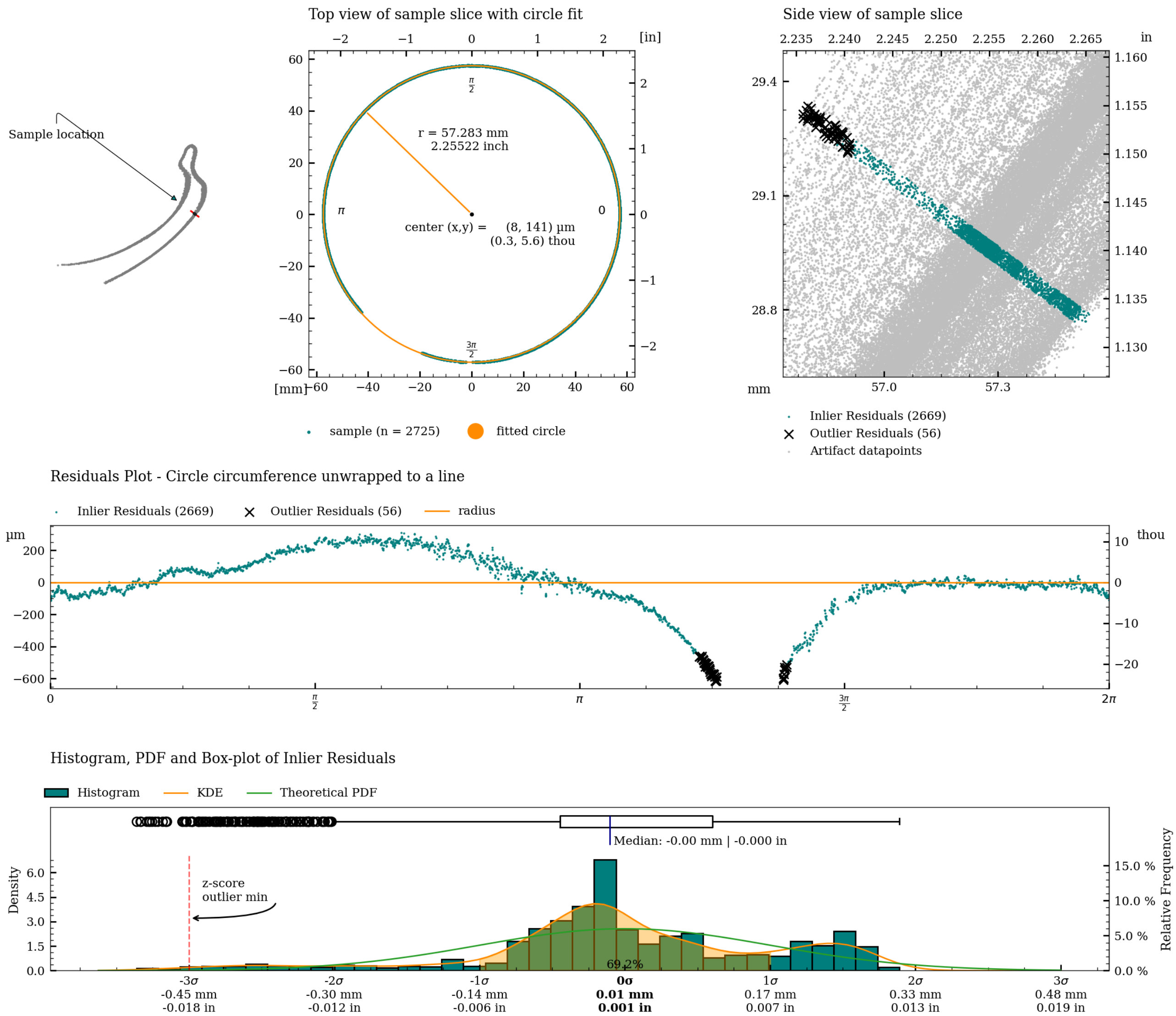

Figure 29: Detailed plot of concentricity measurement for c03.

Concentricity analysis of c04

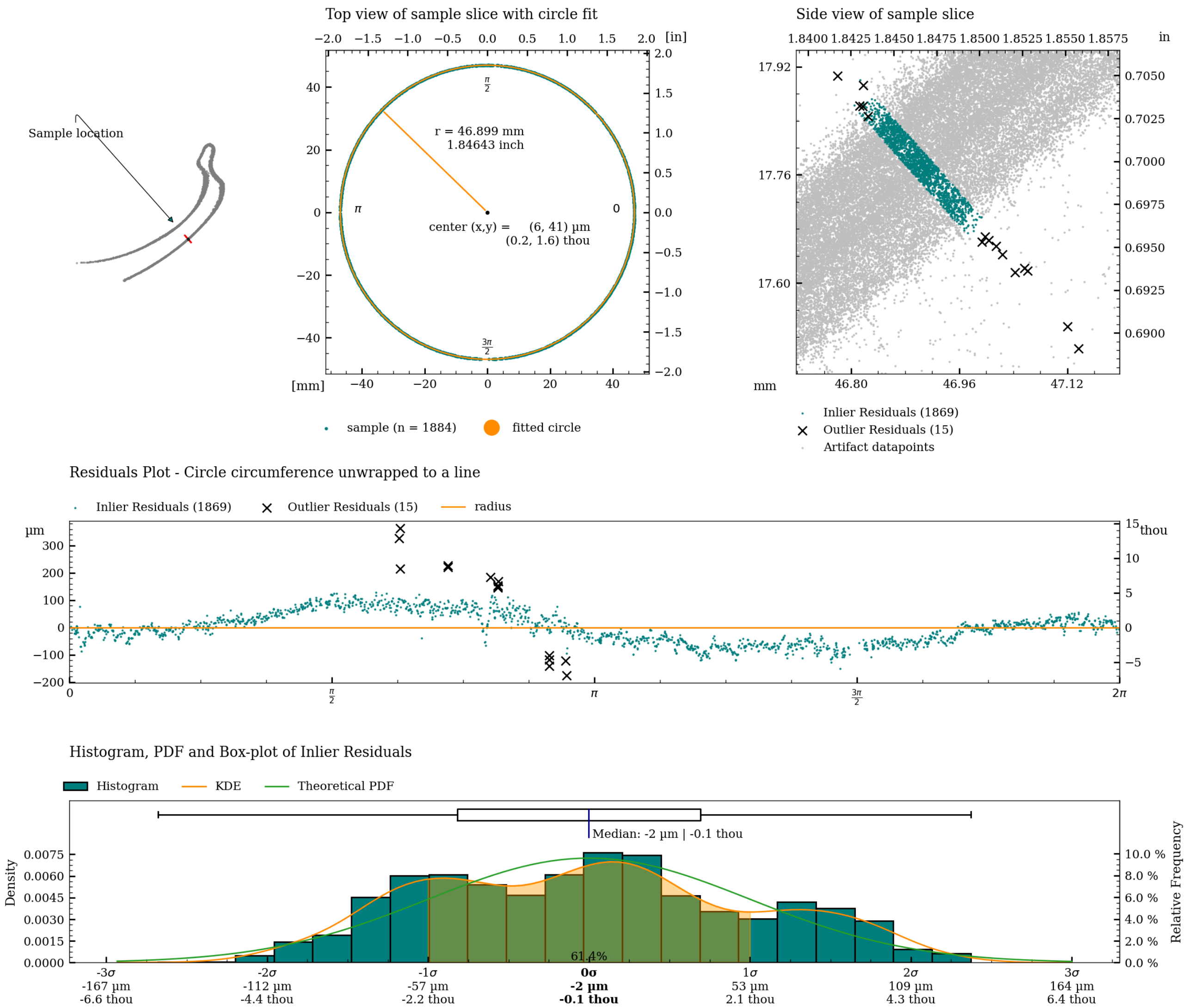

Figure 30: Detailed plot of concentricity measurement for c04.

Concentricity analysis of c05

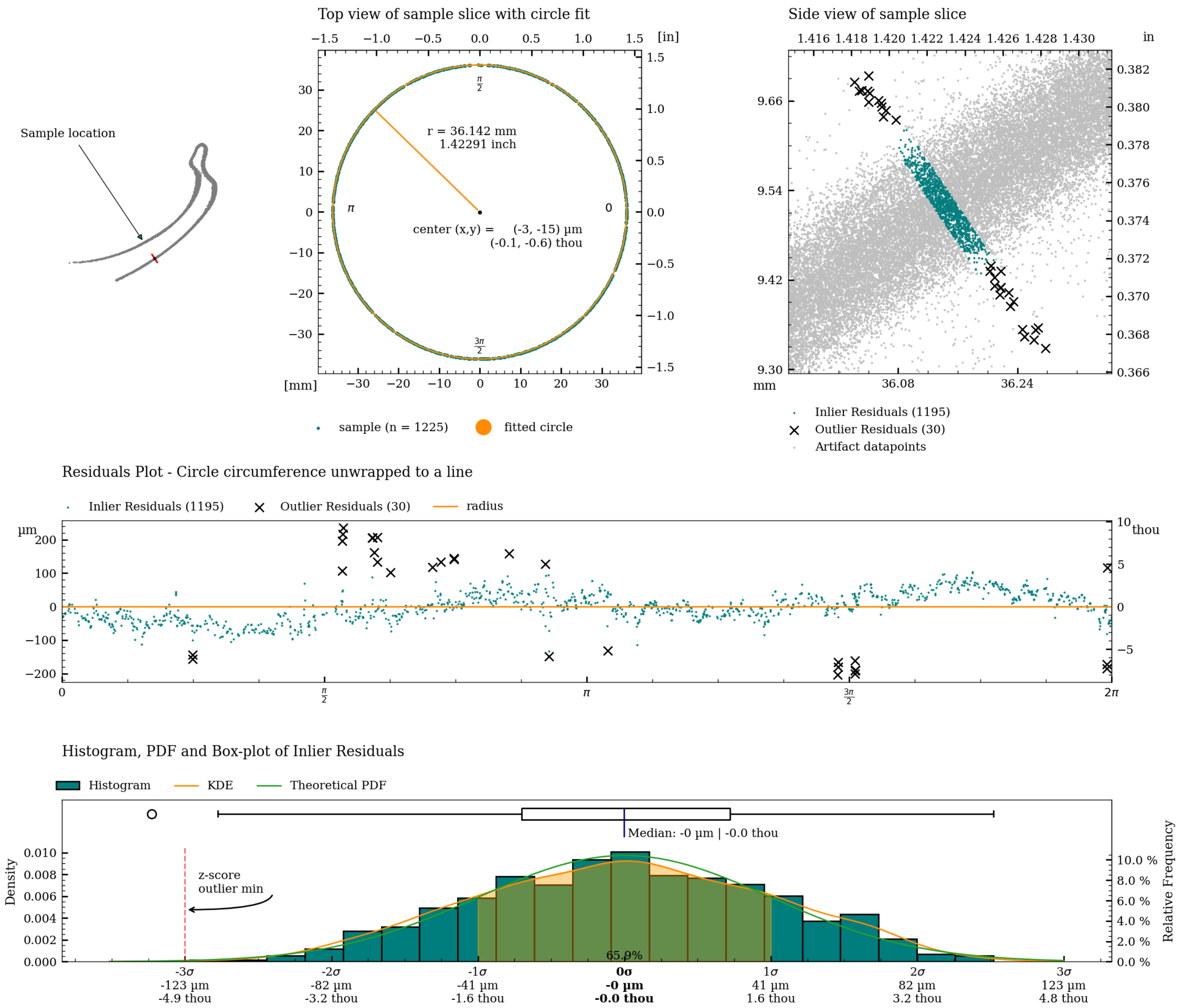

Figure 31: Detailed plot of concentricity measurement for c05.

Concentricity analysis of c06

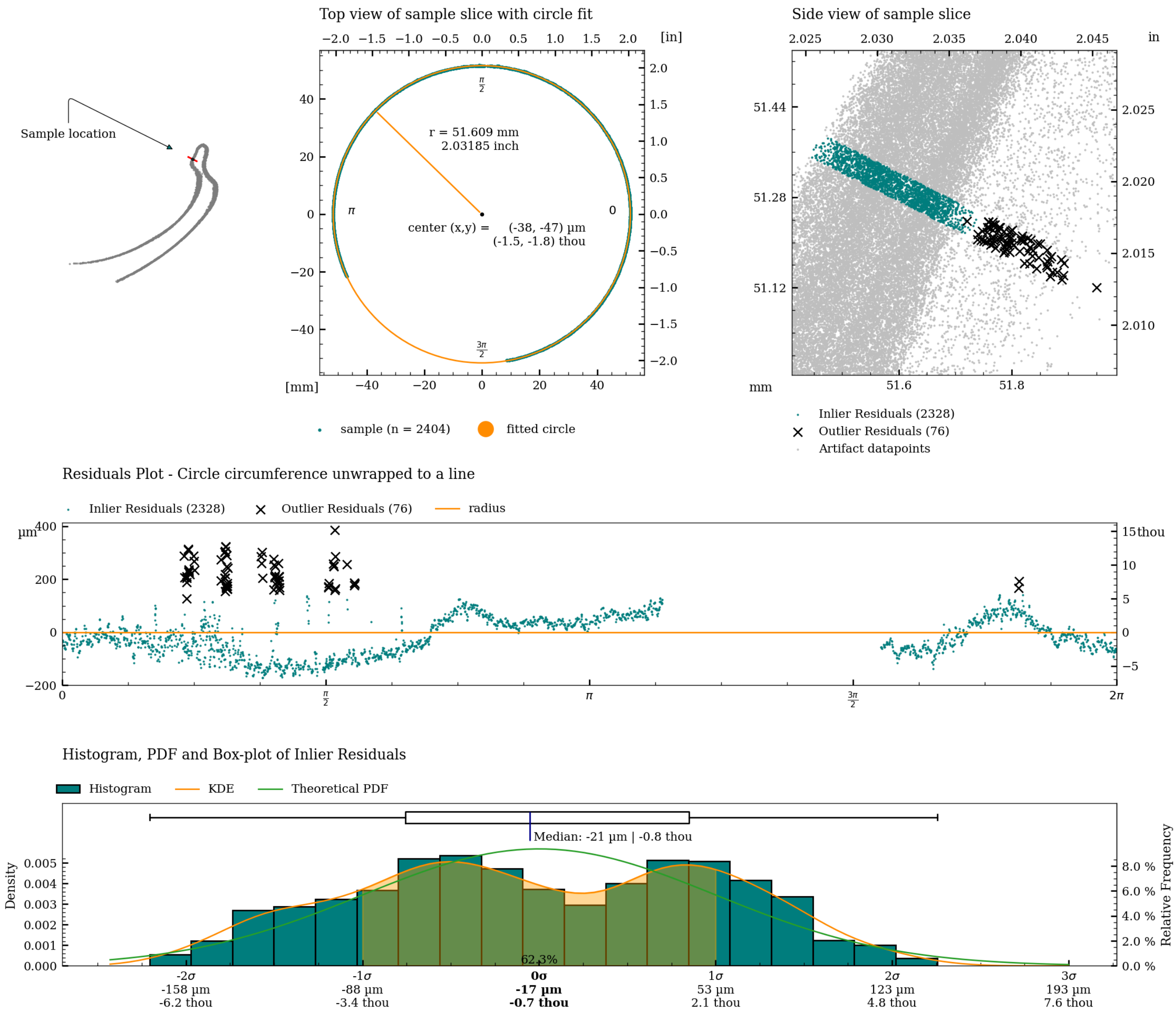

Figure 32: Detailed plot of concentricity measurement for c06.

Concentricity analysis of c07

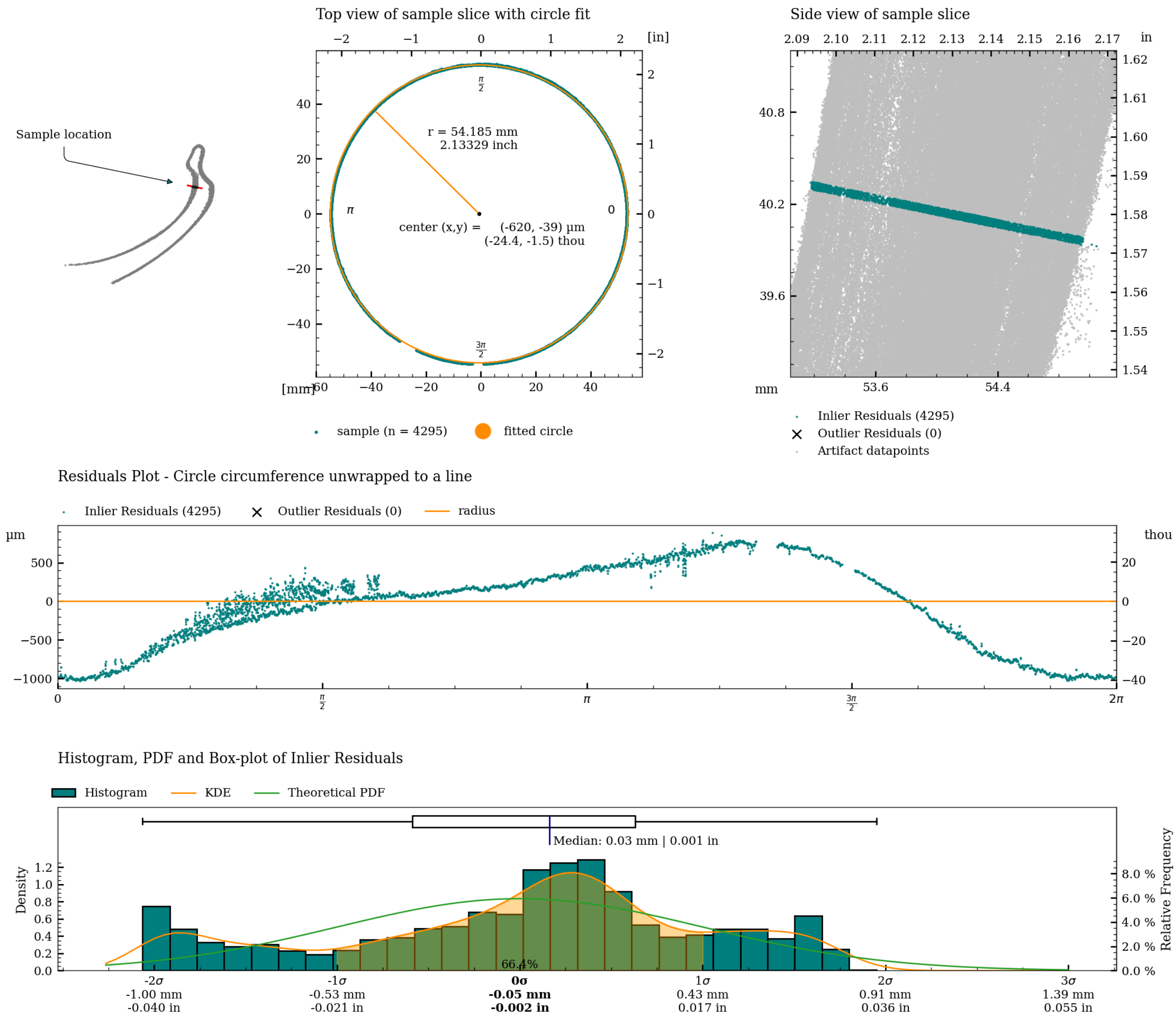

Figure 33: Detailed plot of concentricity measurement for c07.

Concentricity analysis of c08

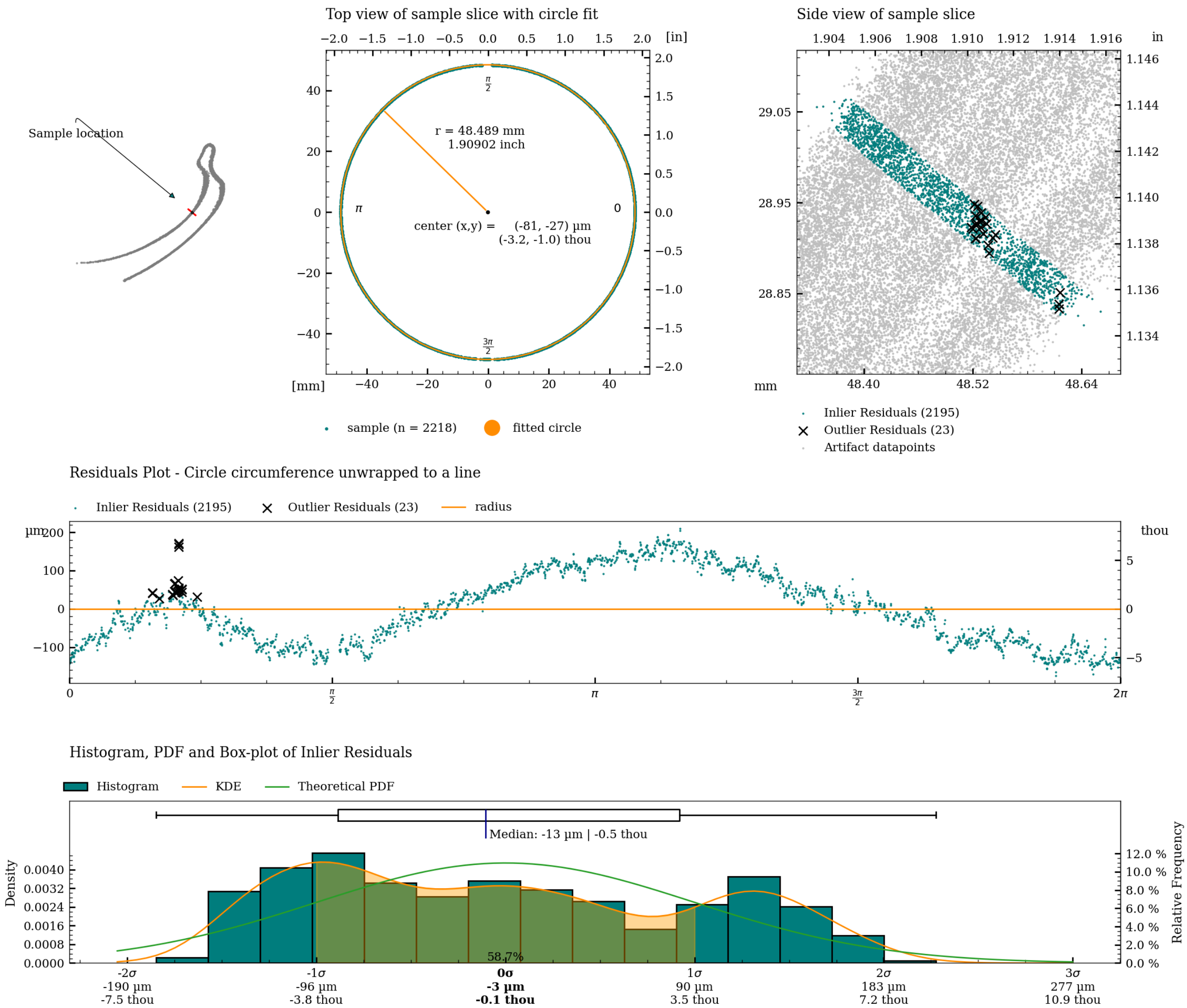

Figure 34: Detailed plot of concentricity measurement for c08.

Concentricity analysis of c09

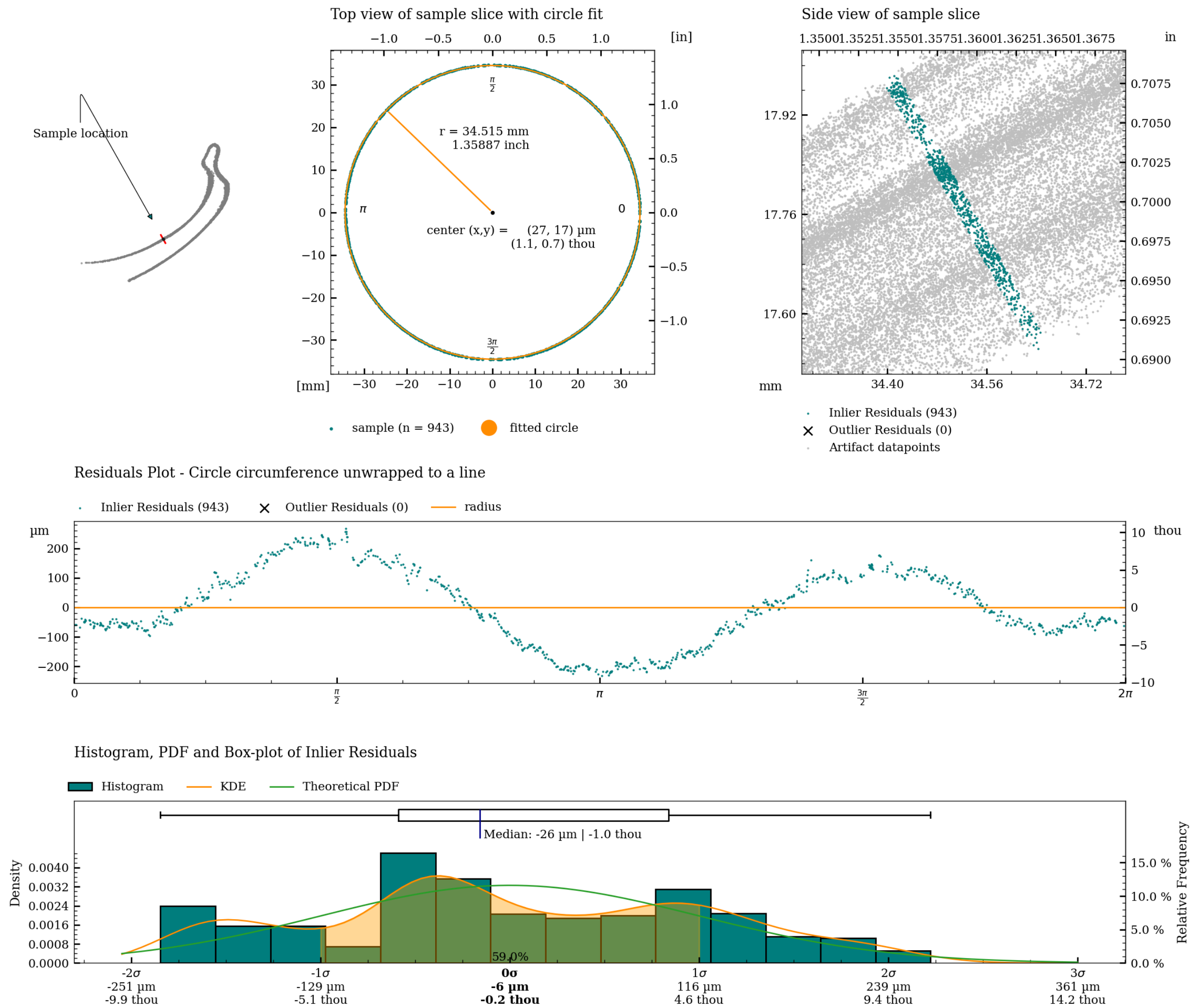

Figure 35: Detailed plot of concentricity measurement for c09.

Concentricity analysis of c10

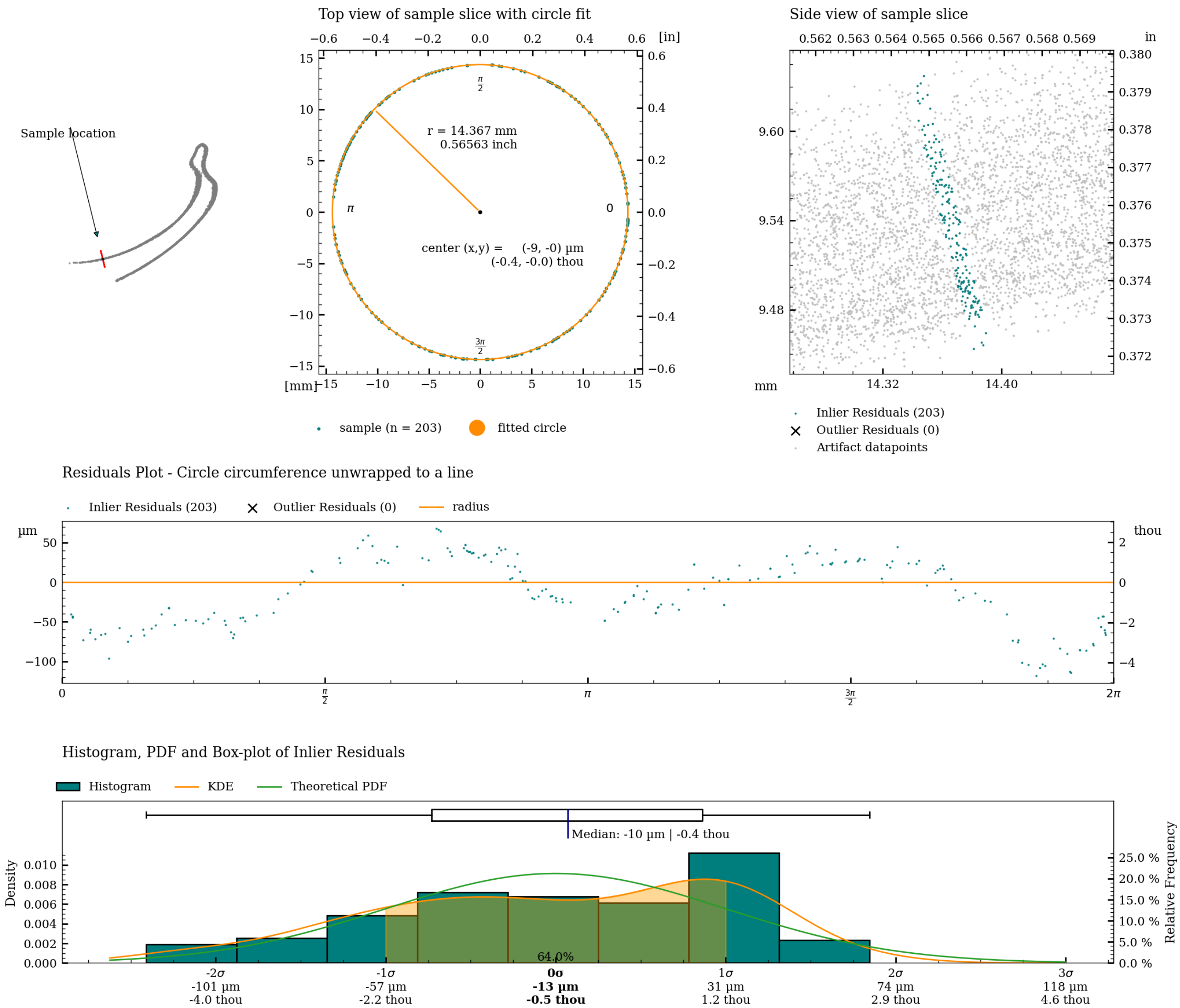

Figure 36: Detailed plot of concentricity measurement for c10.

Coaxiality

Coaxiality is a measure of the deviation in the central axis of an object. Coaxiality measurements are calculated using RANSAC (Random sample consensus) algorithm for outlier detection of a least squares circle regression on cross-sections of the vessel (excluding potential handles) to estimate the best fit circle centers for each slice of the vessel.

Coaxiality is measured for:
- The exterior surface (excluding handles)
- The interior surface

	Exterior		Interior	
Analyzed Slices		1133		944
Median sample size		2379		2263
Slice Height	50 µm	2.0 thou	50 µm	2.0 thou
Statistics with Z-axis as Reference				
Median Absolute Deviation (MAD)	81 µm	3.2 thou	83 µm	3.3 thou
Standard Deviation (SD)	139 µm	5.5 thou	242 µm	9.5 thou
Root Mean Square Deviation (RMSD)	198 µm	7.8 thou	328 µm	12.9 thou
Statistics with Best Fit Central Axis as Reference				
Best fit Central Axis Equation (in metric coordinate system with unit [mm])	x = 0.059 + t-0.00325 y = 0.111 + t-0.00605 z = 0.000 + t0.99998		x = 0.083 + t-0.00813 y = 0.035 + t-0.00224 z = 0.000 + t0.99996	
Axis tilt		−0.187°		−0.467°
Median Absolute Deviation (MAD)	128 µm	5.1 thou	150 µm	5.9 thou
Standard Deviation (SD)	67 µm	2.7 thou	149 µm	5.9 thou
Root Mean Square Deviation (RMSD)	147 µm	5.8 thou	246 µm	9.7 thou

Table 4: Coaxiality analysis of vessel MV009.

Coaxiality plots, exterior surface

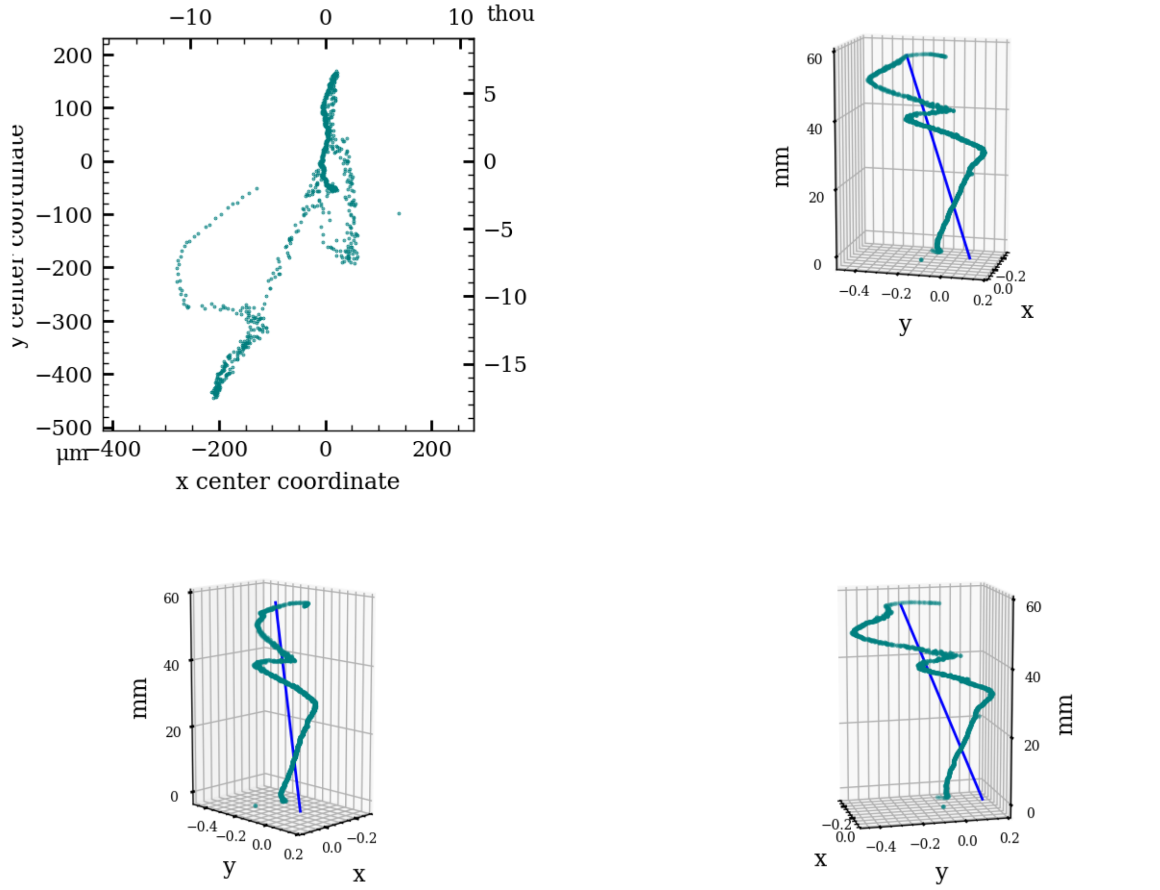

Coaxiality residuals from fitted axis, exterior surface

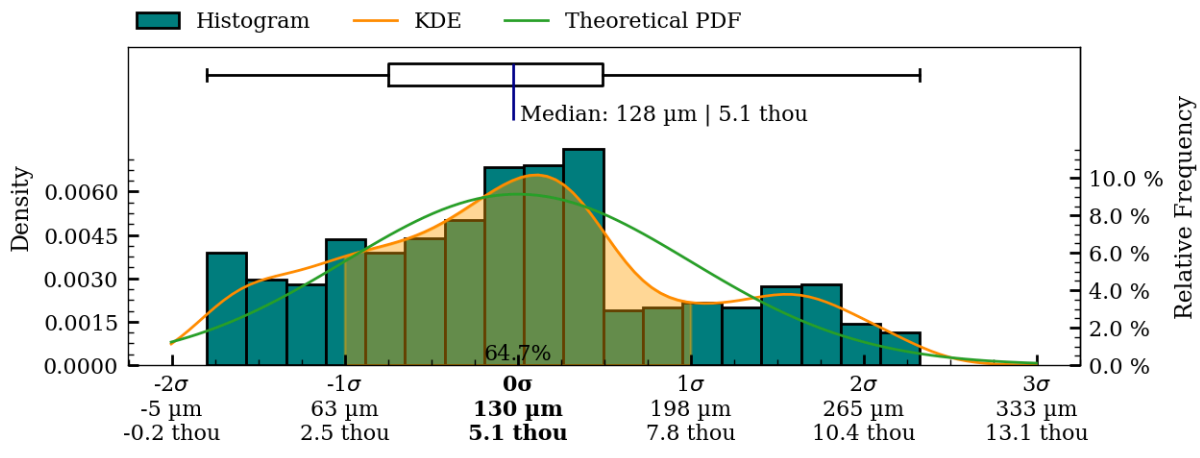

Figure 37: Coaxiality residual plots of exterior surface, MV009.

Coaxiality plots, interior surface

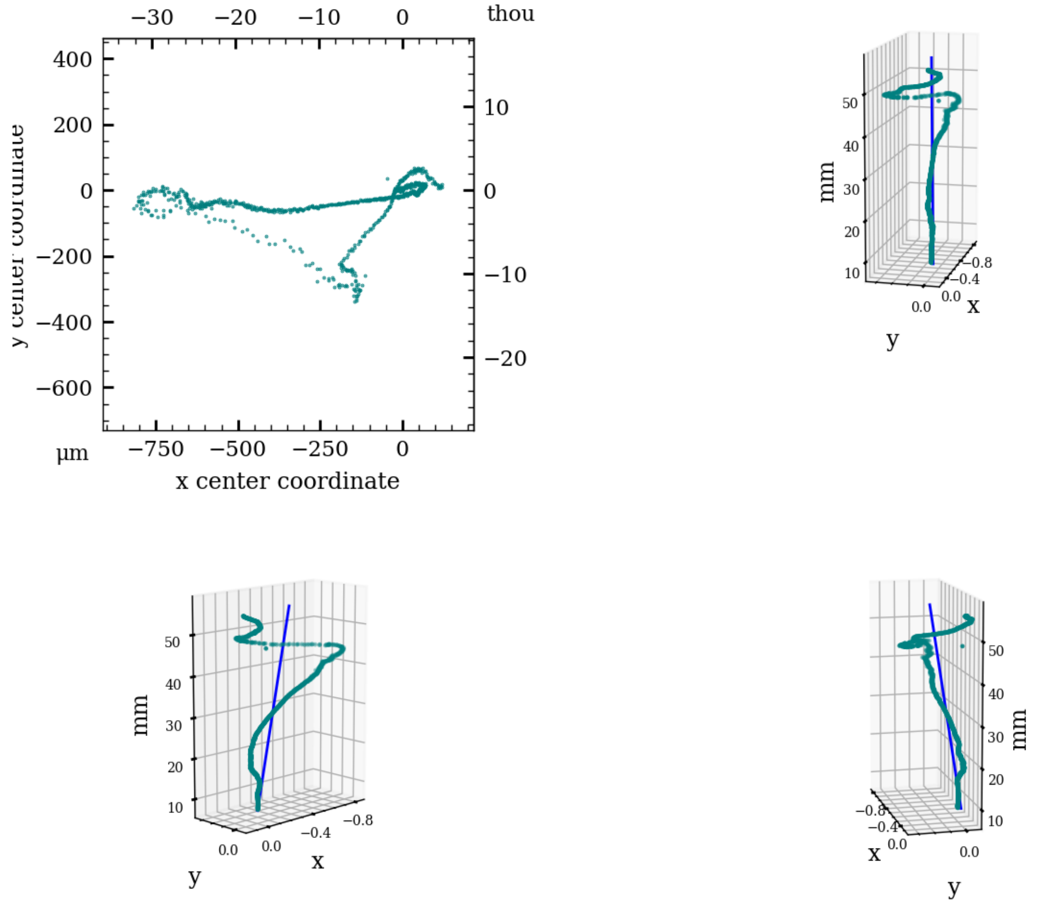

Coaxiality residuals from fitted axis, interior surface

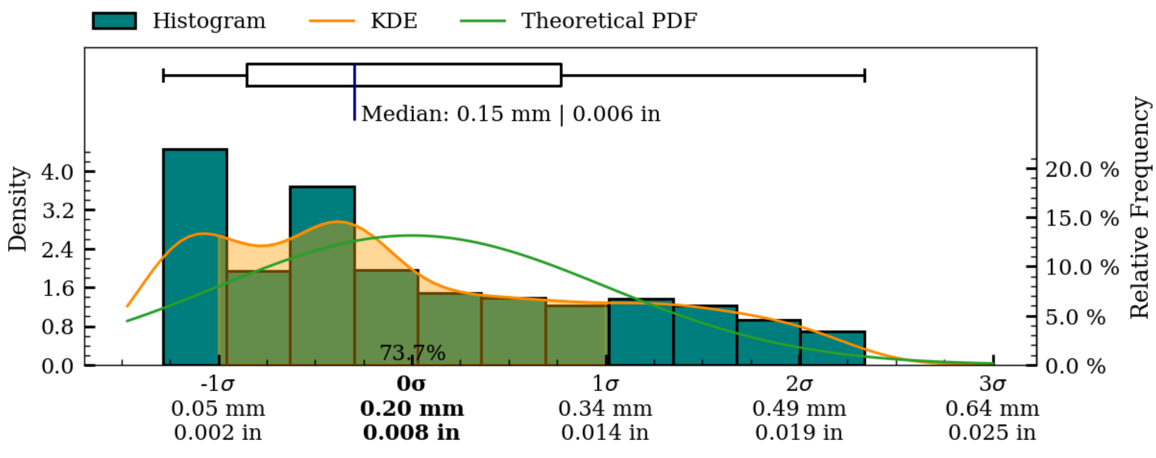

Figure 38: Coaxiality residual plots of interior surface, MV009.

Surface Variability

To illustrate the overall surface deviations of the object, a surface variability heatmap has been created. This heatmap provides an accessible overview of the topography of the manufacturing precision and surface structure of the object.

The surface variability measurements are created by fitting a number of higher-order polynomials to the two-dimensional folded profile of the scan data. This process creates an idealized mathematical representation of actual surface curvature of object, and as such provides a continuous model representation of the actual object. It is important to note that only such a non-discretized representation is sufficient to avoid introducing inconsistently varying errors in the mapping of the final surface deviation results, that the rendered heatmaps are based on.

To produce the final surface variability map, the distance from each scanned vertex to the fitted polynomial is calculated and used as the mapping function input, for applying colours to the surface of the object.

It is important to note that this variability map does not describe deviations from the original *intended* shape of the artifact (if any), as this shape (the *intended design*, so to speak) will have been lost to time. It does however provide a very informative visualization of the texture and structure of the surface and very importantly, *does* hightlight potential manufacturing-relevant patterns in the surface texture (if present). Such patterns are, as an example, clearly evident on the interior surface of artifact PV001.

Exterior surface

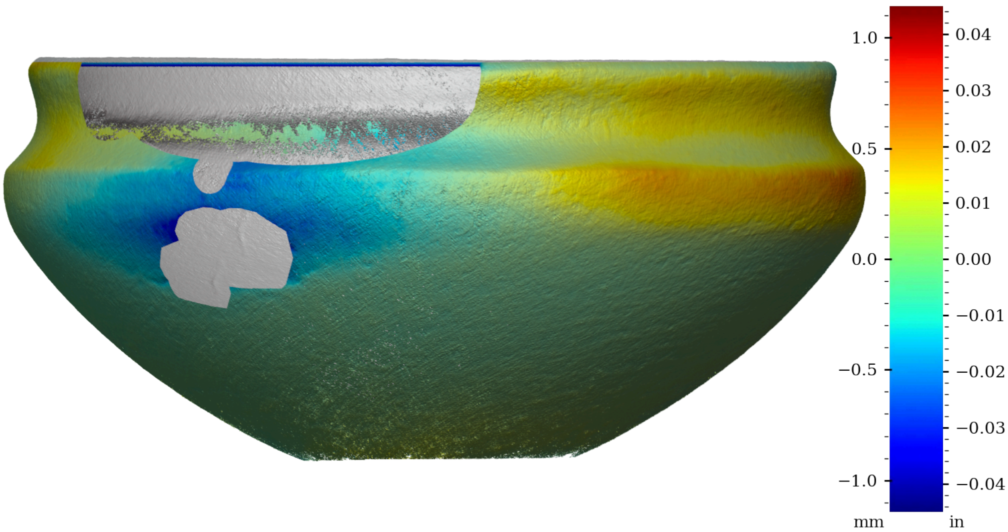

Figure 39: Surface variability heatmap of MV009, front view

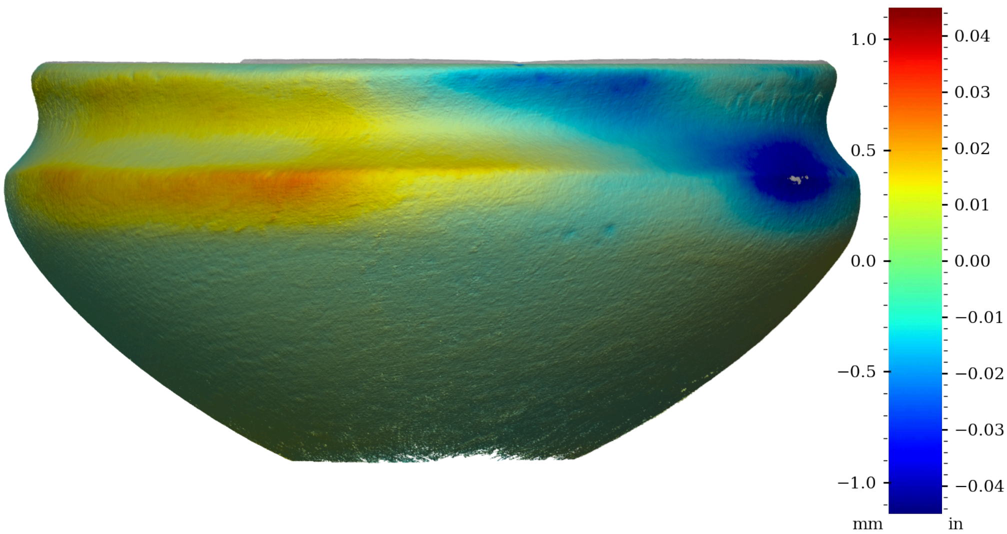

Figure 40: Surface variability heatmap of MV009, rotated 90°

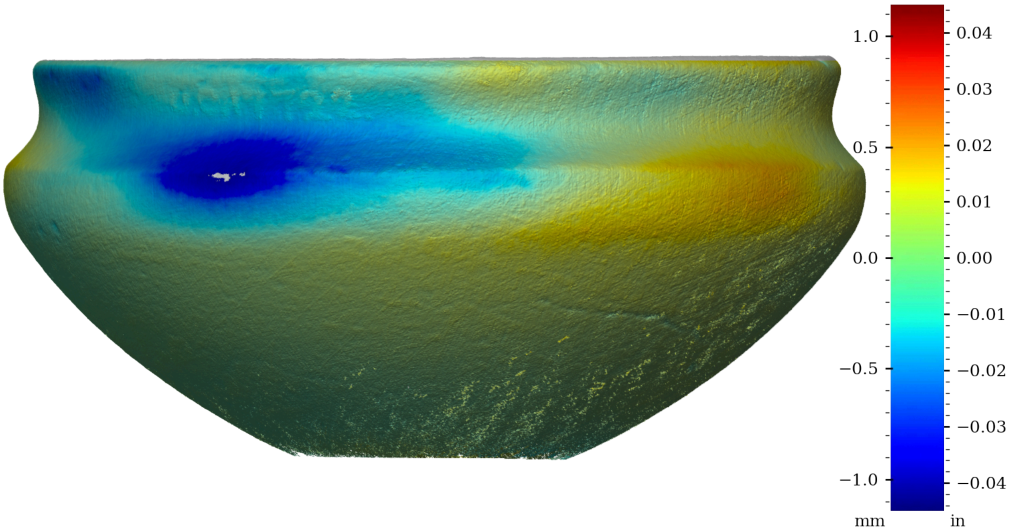

Figure 41: Surface variability heatmap of MV009, rotated 180°

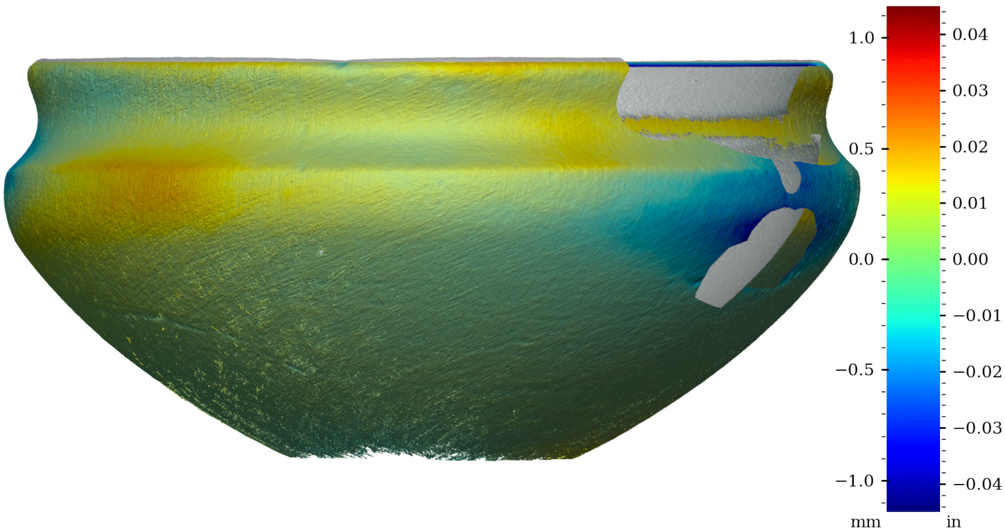

Figure 42: Surface variability heatmap of MV009, rotated 270°

Interior surface

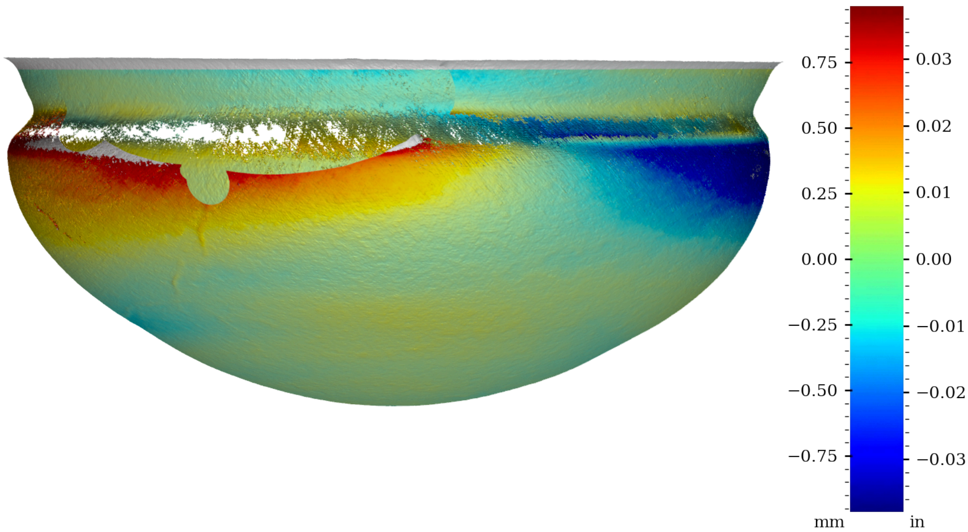

Figure 43: Surface variability heatmap of MV009, front view

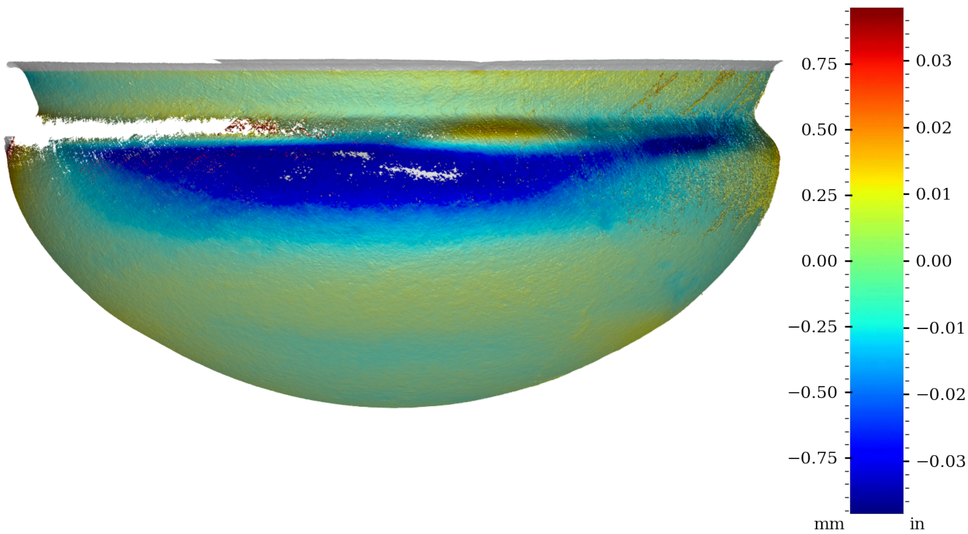

Figure 44: Surface variability heatmap of MV009, rotated 90°

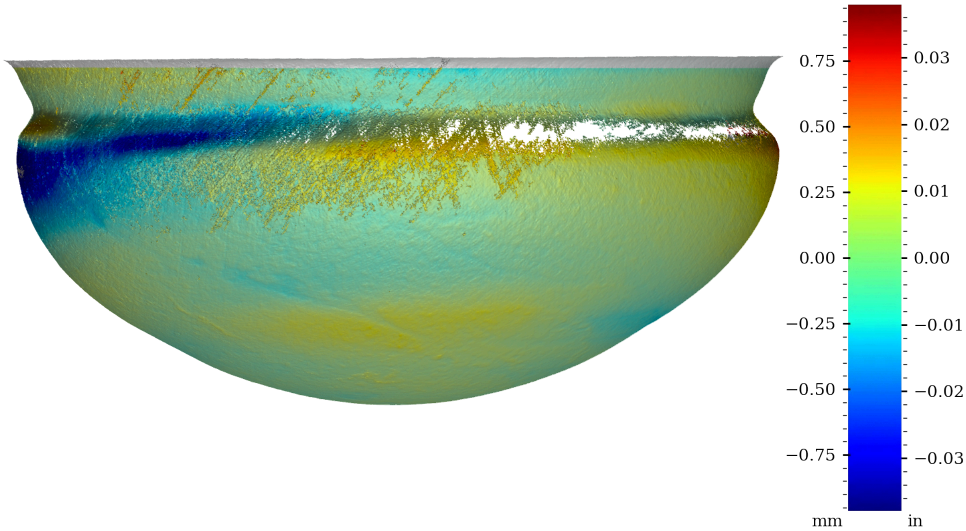

Figure 45: Surface variability heatmap of MV009, rotated 180°

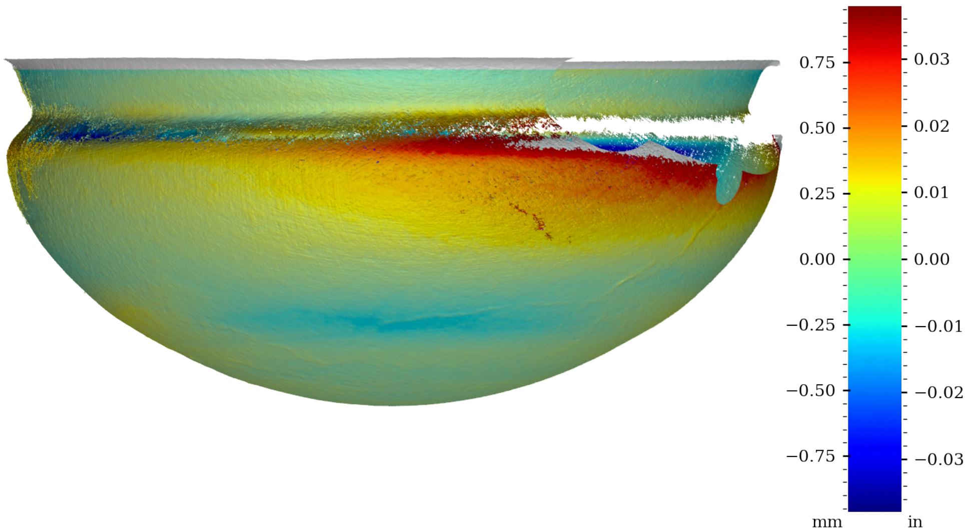

Figure 46: Surface variability heatmap of MV009, rotated 270°

Surface variability statistics

Area	MSD	RMSD	SD	Mean AD	Median AD	Range	Min	Max	Sample size
	mm^2	mm	mm	mm	mm	mm	mm	mm	
Exterior	0.0644	0.254	0.254	0.092	0.169	2.036	−1.218	0.818	4270487
Interior	0.0754	0.275	0.275	0.090	0.175	3.098	−1.133	1.964	3565497
	in^2	in	in	in	in	in	in	in	
Exterior	0.000100	0.0100	0.0100	0.0036	0.0067	0.0801	−0.0479	0.0322	4270487
Interior	0.000117	0.0108	0.0108	0.0036	0.0069	0.1219	−0.0446	0.0773	3565497

Table 5: Surface variability statistics, MV009

Table 5 shows the statistics of the distance from the scan vertices to the best fit object model. These statistics are briefly explained below.

Mean Squared Deviation (MSD), also known as Mean Squared Error (MSE).

$$\mathrm{MSD} = \frac{\sum_{i=1}^{n} (y_i - \hat{y})^2}{n}$$

The MSD metric shows the the average squared difference between the scanned points and the fitted composite polynomial model (a value of 0 would be a perfect match). This metric emphasizes imperfections in the surface of the artifact. Outliers will negatively influence this metric, raising the value of the MSE.

Root Mean Squared Deviation (RMSD), also known as Root Mean Squared Error (RMSE).

$$\mathrm{RMSD} = \sqrt{\frac{\sum_{i=1}^{n} (y_i - \hat{y})^2}{n}}$$

Measures the dispersion of the measured surface variability y_i around a model predictor ($\hat{y}$). By obtaining the root of the MSD, the exponent will be removed from the measurement, enabling comparisons with other statistics of the same unit and making it more accessible to those familiar with the RMSD metric. This measure is used to assess the fit of a regression model to a dataset, in this case our best fit composite polynomial model. The lower the RMSD metric, the better the fit.

Standard Deviation (SD)

$$s = \sqrt{\frac{\sum_{i=1}^{n} (y_i - \bar{y})^2}{n-1}}$$

Measures the dispersion of the measured surface variability y_i around the mean ($\bar{y}$). If the residuals are normally distributed around the mean ($\bar{y} \approx 0$), the SD will be equal to the RMSD. See Figure 47 and Figure 48

Mean Absolute Deviation (MeanAD)

$$\mathrm{MeanAD} = \frac{\sum_{i=1}^{n} |y_i - \bar{y}|}{n}$$

This metric is similar to the SD, but the difference between the residuals and the mean is *not* squared. Instead of indicating the spread of the data, we look at the average distance between each data point and the mean. The Mean Absolute Deviation is affected less by outliers than the Standard Deviation.

Median Absolute Deviation (MedianAD)

$$\mathrm{MedianAD} = \mathrm{median}(|y_i - \mathrm{median}(y)|)$$

The Median Absolute Deviation is measure of the dispersion of the data around the median.

Range

$$\max(y_i) - \min(y_i)$$

Range is a measure of the total spread of the residuals

Histogram, KDE and Box-plot of measured surface variability - exterior surface

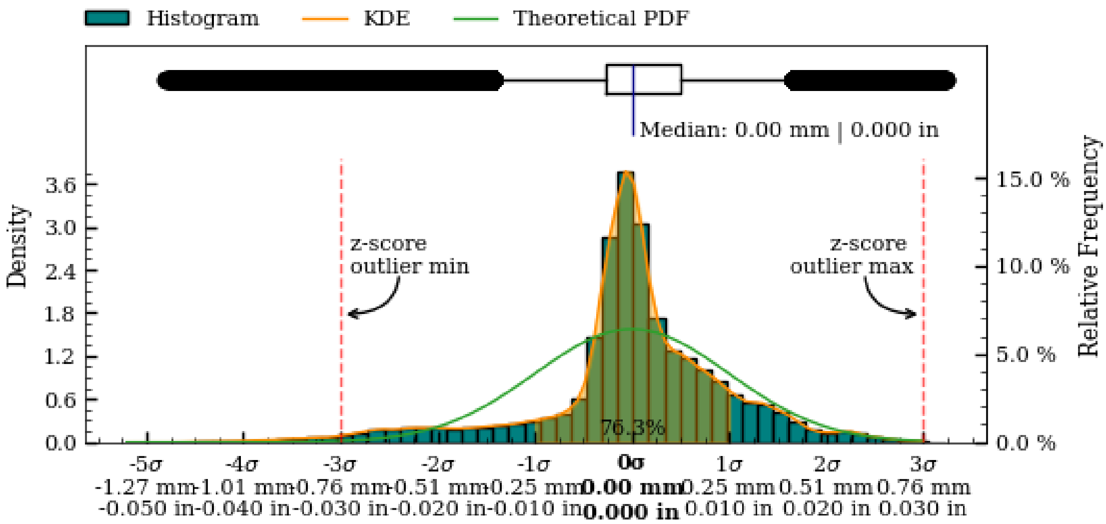

Figure 47: Exterior surface variability boxplot, kds and histogram.

Histogram, KDE and Box-plot of measured surface variability - interior surface

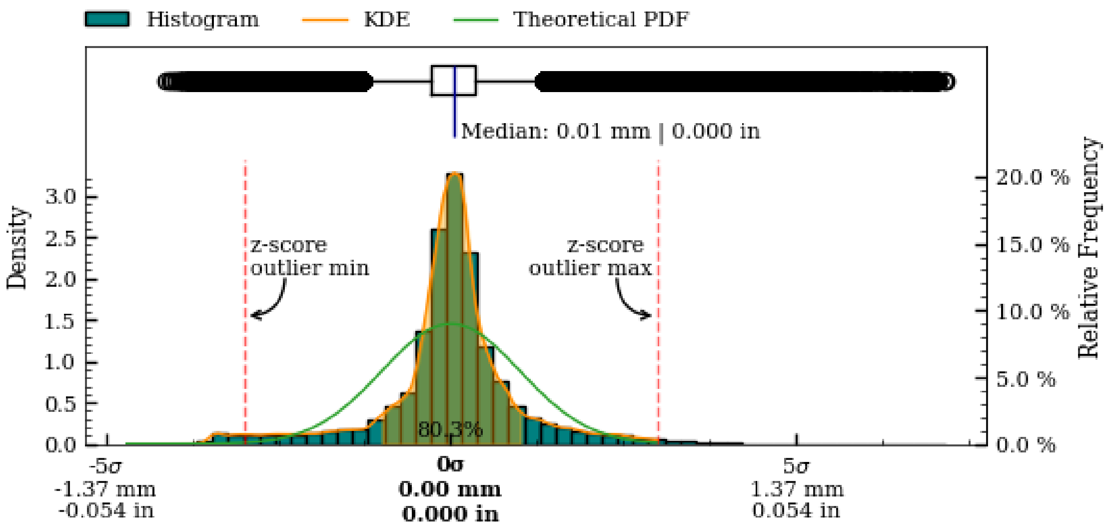

Figure 48: Interior surface variability boxplot, kds and histogram.

Precision Score Of The Artifact

To enable valid comparison of the manufacturing precision of different artifacts, a metric that robustly quantifies the overall precision of the object is required. The considerations for such a metric will be explored in this section.

Based on these considerations, a *Precision Score* metric will be defined.

For an object to be described as having been manufactured with high precision, several qualities must be present *concurrently*, and throughout the *entire* geometry of the final object. A given object may exhibit high levels of one or more *components* of precision, but be lacking in others. For example:

- An object may present high levels of coaxialility, but lack circularity.
- An object may exhibit good circularity, but show imperfections in the surface structure.
- An object may be smoothed to perfection *without* any circularity or coaxiality.
- An object may exhibit high levels of all of the above metrics in *some* areas, but not in others.

Therefore, a precision score metric **must** account for *all* aspects of the individual, underlying precision metrics (circularity, concentricity, coaxiality and surface variability) throughout the *entire* surface area of the object.

The composite high order polynomial model, used to generate the surface variability map (described in Surface Variability, p. 41) is the best continuous mathematical representation of the object available to us (lacking any original design plans, as would normally be available in metrological analysis). This idealized model encompasses all of the above component metrics.

In the creation of the model, all scan data-points are taken into account (excluding areas with extensive damage), making it the best possible idealized representation we can achieve. When this model has been accurately created, the deviation between the model and the scanned data-points can be calculated over the non-discretized polynomials, *without* the need for an "original" CAD model (and importantly, unless such a CAD model *actually* corresponded to the original design intent, it would be an insufficient comparison basis).

Within the context of defining a valid, overall precision metric, this approach satisfies the incorporation of all of the necessary metrics:

- **Circularity**: Because the reconstructed polynomial model is revolved around the Z-plane, the idealized representation is perfectly circular, and thus incorporates the circularity component.
- **Concentricity and coaxiality**: Because the Z-axis (datum axis) is the center axis of the model, it incorporates the concentricity and coaxiality components.
- **Surface variability**: Because the model is continuous and non-discretized, it can be used accurately for all points of the scan data, and incorporates the surface variability component.

The level of precision ultimately achieved in a physical object does not share a linear relationship with its manufacturing requirements. Since continuously higher levels of final precision becomes progressively harder to achieve, an overall precision metric must take this relationship into account.

A robust statistical metric that satisfies this requirement is the *Mean Squared Deviation* (MSD or MSE). Here specifically, we can utilize the mean square of the deviations between the model ($\hat{y}$) and the data-points (y_i).

Combining all of the above considerations, we can express a well-defined *Precision Score* metric, that provides an immediately accessible way to understand the overall precision of an object, while being statistically valid. Since the Mean Squared Deviation tends towards zero as the overall precision increases, the inverse of the Mean Squared Deviation is taken to obtain a precision score metric that increases as precision increases[12]:

$$\text{Precision Score} = \frac{n}{\sum_{i=1}^{n} (y_i - \hat{y})^2}$$

[12]The precision score unit is $\frac{1}{\text{mm}^2}$

A precision score will be calculated seperately for:

- The exterior surface
- The interior surface
- The full surface

As most scans do not include sufficient scan data for the interior surface, the exterior surface will be used for calculating the precision score in most cases. In the rare case that the scan data is more complete for the *interior* surface, this will be used instead.

Table 6 shows the precision score of this artifact (MV009), compared to the two most precise, and the two least precise vessels currently analyzed.

Artifact			**Material**	**Precision Score**	**Link to Report**
	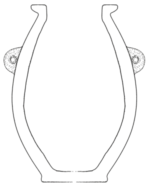	PV001	Red Granite	**1905** Full: 980 Exterior: 1905 Interior: 705	Report Publication
	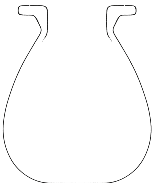	PV006	Dark grey granite	**621** Full: 521 Exterior: 621 Interior: 152	Report Publication
	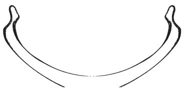	MV009	Diorite	**16** Full: 14 Exterior: 16 Interior: 13	Report Publication
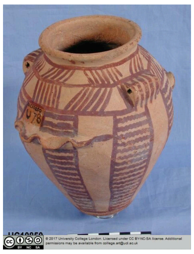	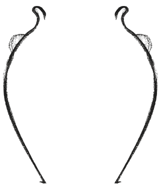	MV001	Pottery	**1.93** Full: 1.92 Exterior: 1.93 Interior: 1.85	Report Publication
	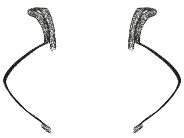	MV010	Calcite (Egyptian Alabaster)	**1.12** Full: 0.64 Exterior: 1.12 Interior: 0.20	Report Publication

Analysis Roadmap

While the current iteration of this work already provides valuable results, continued future additions and improvements will enhance their utility further. This section details planned iterative updates and improvements, to both the reports themselves, and to the underlying methodology and software they are created with.

Alignment Section

- Detailed exploration of different circle regression algorithms
- If handles are present on the vessel, exploring alignment of the vessels so the handle positions match each other
- Add optimization of the perpendicular surface deviation, with the best results of the coaxial alignment
- Align by minimizing circularity results (of rotated sample slice, to compensate for sample height distortions)

Measurements of Precision

- Section detailing how measurements perpendicular to the surface curvature are obtained
- Detailed surface area analysis, exploring the residual patterns throughout subsequent sample slices of the artifact surface
- Wall thickness deviation color map
- Robust outlier identification on circularity, to better handle analysis of damaged areas of the artifacts in addition to removal of interior crystalline structure points present in CT scans
- Layout updates to the charts and tables

Visibility of Outliers and Damaged Sections

- Identification and marking of damaged parts
- Visualization of outliers on the artifact surface

Exploration of Mathematical Primitives

- Analysis of selected curvatures and flat surfaces on the vessel in both the horizontal and vertical planes
  - Circles
  - Parabolas
  - Ellipsoids
  - Hyperbolas
  - Cones
- Implementation of robust regressions models suitable for this domain, based on RANSAC.

Metrics on Primary Features

- Measurements of features in the horizontal plane
- Measurements of features in the vertical plane
- Measurements of angles
- Measurements of volume

Exploration of Potential Design Ratios

- π, φ, e, 1, 2, 3, 4 etc.

Raw Dataset Attachments

- Including all measurement and sample coordinates as CSV-files embedded in the report
- Including an STL file of the aligned object alongside the report, for easier external replication and validation of the research results

Appendix A - Comparison Of Circularity Measurements (Z-plane vs. surface-perpendicular)

Comparison of circularity samples

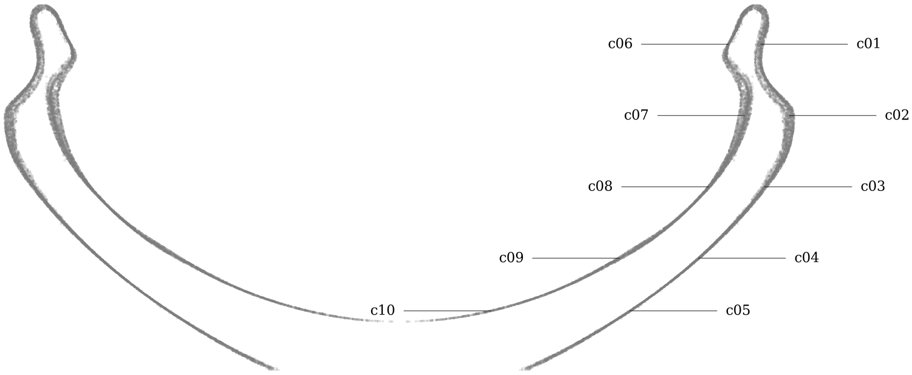

Samples perpendicular to the surface curvature

Tag	Area	Measured deviation[8]	Residuals				Sample size	Slice		
			Range	RMSD[9]	MAD[10]	SD		Height	Z coord.	Radius[11]
		mm	mm	mm	mm	mm		mm	mm	mm
c01	exterior	Ø113.246±0.701	1.175	0.310	0.268	0.310	2726	0.050	51.298	56.623
c02	exterior	Ø122.202±1.178	1.981	0.492	0.413	0.492	3558	0.050	40.124	61.101
c03	exterior	Ø114.578±0.622	0.924	0.173	0.077	0.173	2725	0.050	28.951	57.289
c04	exterior	Ø93.801±0.362	0.539	0.058	0.043	0.058	1884	0.050	17.777	46.900
c05	exterior	Ø72.286±0.234	0.439	0.048	0.030	0.048	1225	0.050	9.520	36.143
c06	interior	Ø103.201±0.392	0.557	0.081	0.058	0.081	2404	0.050	51.298	51.601
c07	interior	Ø108.287±0.993	1.918	0.478	0.294	0.478	4295	0.050	40.124	54.144
c08	interior	Ø96.987±0.206	0.384	0.093	0.086	0.093	2218	0.050	28.951	48.494
c09	interior	Ø69.036±0.265	0.499	0.123	0.088	0.123	943	0.050	17.777	34.518
c10	interior	Ø28.742±0.120	0.186	0.046	0.034	0.044	203	0.050	9.520	14.371

Table 7: Detailed circularity measurements at selected samples in z-plane, vessel MV009.

Samples in the Z-plane

Tag	Area	Measured deviation[8]	Residuals				Sample size	Slice		
			Range	RMSD[9]	MAD[10]	SD		Height	Z coord.	Radius[11]
		mm	mm	mm	mm	mm		mm	mm	mm
c01	exterior	Ø113.358±0.769	1.208	0.327	0.239	0.323	2827	0.050	51.298	56.679
c02	exterior	Ø122.446±1.310	2.003	0.515	0.404	0.502	3528	0.050	40.124	61.223
c03	exterior	Ø114.563±0.741	1.155	0.211	0.096	0.211	4091	0.050	28.951	57.281
c04	exterior	Ø93.787±0.427	0.741	0.087	0.064	0.087	4233	0.050	17.777	46.894
c05	exterior	Ø72.278±0.500	0.932	0.085	0.055	0.085	3988	0.050	9.520	36.139
c06	interior	Ø103.177±0.512	0.715	0.101	0.066	0.100	3074	0.050	51.298	51.589
c07	interior	Ø108.439±1.074	1.869	0.498	0.298	0.492	4504	0.050	40.124	54.220
c08	interior	Ø96.966±0.283	0.502	0.122	0.105	0.122	3744	0.050	28.951	48.483
c09	interior	Ø68.943±0.636	1.070	0.249	0.198	0.246	4156	0.050	17.777	34.471
c10	interior	Ø28.648±0.543	1.050	0.191	0.144	0.191	3525	0.050	9.520	14.324

Table 8: Detailed circularity measurements at selected samples perpendicular to vessel curvature, vessel MV009.

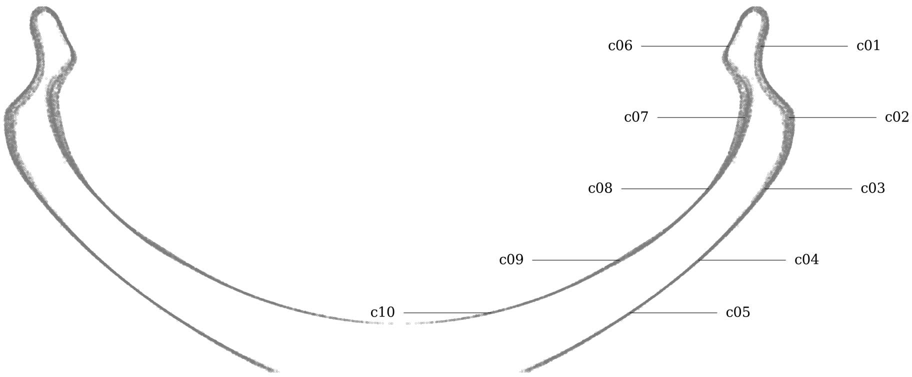

Samples perpendicular to the surface curvature

Tag	Area	Measured deviation[8]	Residuals				Sample size	Slice		
			Range	RMSD[9]	MAD[10]	SD		Height	Z coord.	Radius[11]
		in	in	in	in	in		in	in	in
c01	exterior	Ø4.4585±0.0276	0.0463	0.0122	0.0106	0.0122	2726	0.0020	2.0196	2.2293
c02	exterior	Ø4.8111±0.0464	0.0780	0.0194	0.0163	0.0194	3558	0.0020	1.5797	2.4056
c03	exterior	Ø4.5109±0.0245	0.0364	0.0068	0.0030	0.0068	2725	0.0020	1.1398	2.2555
c04	exterior	Ø3.6929±0.0142	0.0212	0.0023	0.0017	0.0023	1884	0.0020	0.6999	1.8465
c05	exterior	Ø2.8459±0.0092	0.0173	0.0019	0.0012	0.0019	1225	0.0020	0.3748	1.4229
c06	interior	Ø4.0630±0.0154	0.0219	0.0032	0.0023	0.0032	2404	0.0020	2.0196	2.0315
c07	interior	Ø4.2633±0.0391	0.0755	0.0188	0.0116	0.0188	4295	0.0020	1.5797	2.1316
c08	interior	Ø3.8184±0.0081	0.0151	0.0037	0.0034	0.0037	2218	0.0020	1.1398	1.9092
c09	interior	Ø2.7180±0.0104	0.0196	0.0048	0.0035	0.0048	943	0.0020	0.6999	1.3590
c10	interior	Ø1.1316±0.0047	0.0073	0.0018	0.0013	0.0017	203	0.0020	0.3748	0.5658

Table 9: Detailed circularity measurements at selected samples in z-plane, vessel MV009.

Samples in the Z-plane

Tag	Area	Measured deviation[8]	Residuals				Sample size	Slice		
			Range	RMSD[9]	MAD[10]	SD		Height	Z coord.	Radius[11]
		in	in	in	in	in		in	in	in
c01	exterior	Ø4.4629±0.0303	0.0475	0.0129	0.0094	0.0127	2827	0.0020	2.0196	2.2315
c02	exterior	Ø4.8207±0.0516	0.0789	0.0203	0.0159	0.0197	3528	0.0020	1.5797	2.4104
c03	exterior	Ø4.5103±0.0292	0.0455	0.0083	0.0038	0.0083	4091	0.0020	1.1398	2.2552
c04	exterior	Ø3.6924±0.0168	0.0292	0.0034	0.0025	0.0034	4233	0.0020	0.6999	1.8462
c05	exterior	Ø2.8456±0.0197	0.0367	0.0034	0.0022	0.0034	3988	0.0020	0.3748	1.4228
c06	interior	Ø4.0621±0.0202	0.0281	0.0040	0.0026	0.0040	3074	0.0020	2.0196	2.0310
c07	interior	Ø4.2693±0.0423	0.0736	0.0196	0.0117	0.0194	4504	0.0020	1.5797	2.1346
c08	interior	Ø3.8176±0.0112	0.0198	0.0048	0.0041	0.0048	3744	0.0020	1.1398	1.9088
c09	interior	Ø2.7143±0.0251	0.0421	0.0098	0.0078	0.0097	4156	0.0020	0.6999	1.3571
c10	interior	Ø1.1279±0.0214	0.0414	0.0075	0.0057	0.0075	3525	0.0020	0.3748	0.5639

Table 10: Detailed circularity measurements at selected samples perpendicular to vessel curvature, vessel MV009.

Comparison of circularity on the full vessel surface

Metric

Samples perpendicular to the surface curvature

Area	Range			Standard Deviation			Medan Absolute Deviation			Slices	Slice height
	Median	Min.	Max.	Median	Min.	Max.	Median	Min.	Max.		
	mm	mm	mm	mm	mm	mm	mm	mm	mm		mm
Exterior	0.938	0.268	1.989	0.165	0.035	0.499	0.051	0.022	0.426	1133	0.050
Interior	0.665	0.151	2.442	0.141	0.036	0.634	0.058	0.020	0.604	944	0.050

Table 11: Detailed circularity measurements at selected samples in z-plane, vessel MV009.

Samples in the z-plane

Area	Range			Standard Deviation			Medan Absolute Deviation			Slices	Slice height
	Median	Min.	Max.	Median	Min.	Max.	Median	Min.	Max.		
	mm	mm	mm	mm	mm	mm	mm	mm	mm		mm
Exterior	1.160	0.508	2.208	0.250	0.059	0.597	0.070	0.037	0.422	1135	0.050
Interior	1.077	0.395	3.423	0.212	0.073	0.648	0.068	0.040	0.615	960	0.050

Table 12: Detailed circularity measurements at selected samples perpendicular to vessel curvature, vessel MV009.

Imperial

Samples perpendicular to the surface curvature

Area	Range			Standard Deviation			Medan Absolute Deviation			Slices	Slice height
	Median	Min.	Max.	Median	Min.	Max.	Median	Min.	Max.		
	in	in	in	in	in	in	in	in	in		in
Exterior	0.938	0.268	1.989	0.165	0.035	0.499	0.051	0.022	0.426	1133	0.050
Interior	0.665	0.151	2.442	0.141	0.036	0.634	0.058	0.020	0.604	944	0.050

Table 13: Detailed circularity measurements at selected samples in z-plane, vessel MV009.

Samples in the z-plane

Area	Range			Standard Deviation			Medan Absolute Deviation			Slices	Slice height
	Median	Min.	Max.	Median	Min.	Max.	Median	Min.	Max.		
	in	in	in	in	in	in	in	in	in		in
Exterior	1.160	0.508	2.208	0.250	0.059	0.597	0.070	0.037	0.422	1135	0.050
Interior	1.077	0.395	3.423	0.212	0.073	0.648	0.068	0.040	0.615	960	0.050

Table 14: Detailed circularity measurements at selected samples perpendicular to vessel curvature, vessel MV009.

Circularity analysis of exterior samples perpendicular to surface curvature

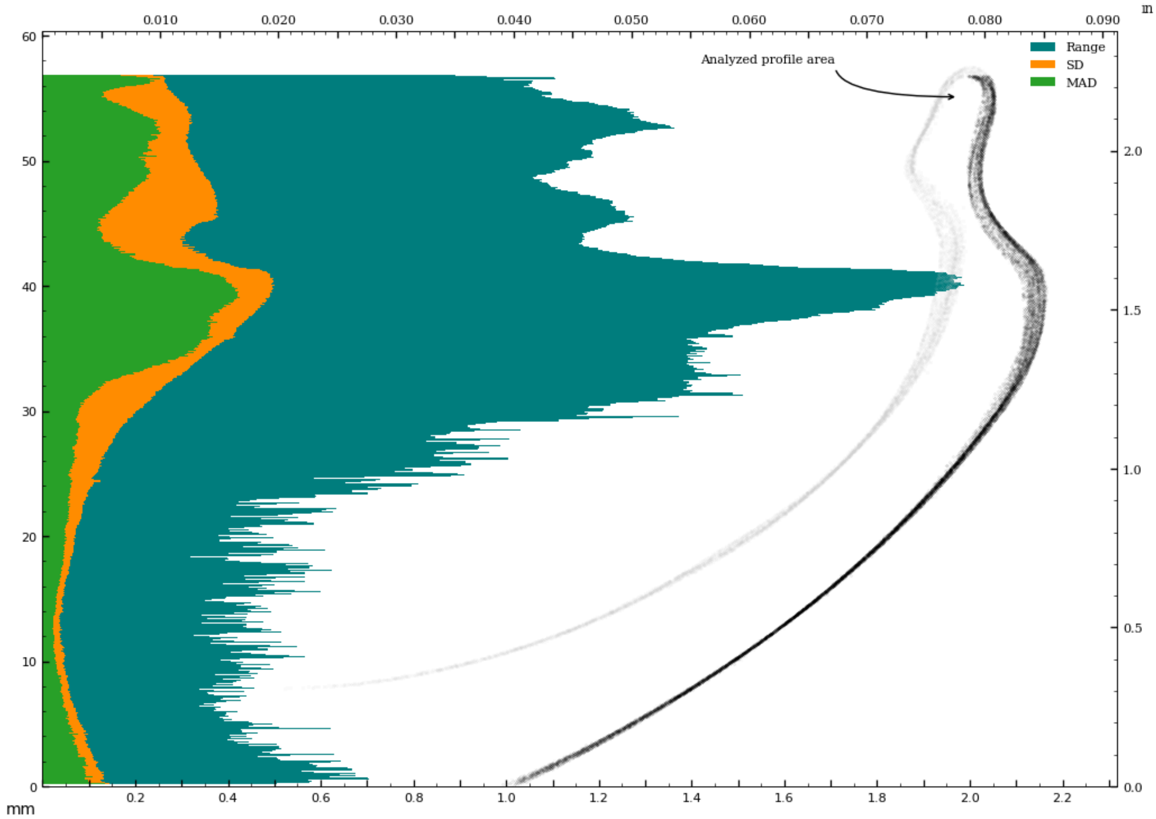

Figure 49: Circularity analysis of exterior samples perpendicular to surface curvature

Circularity analysis of exterior surface - in z-plane

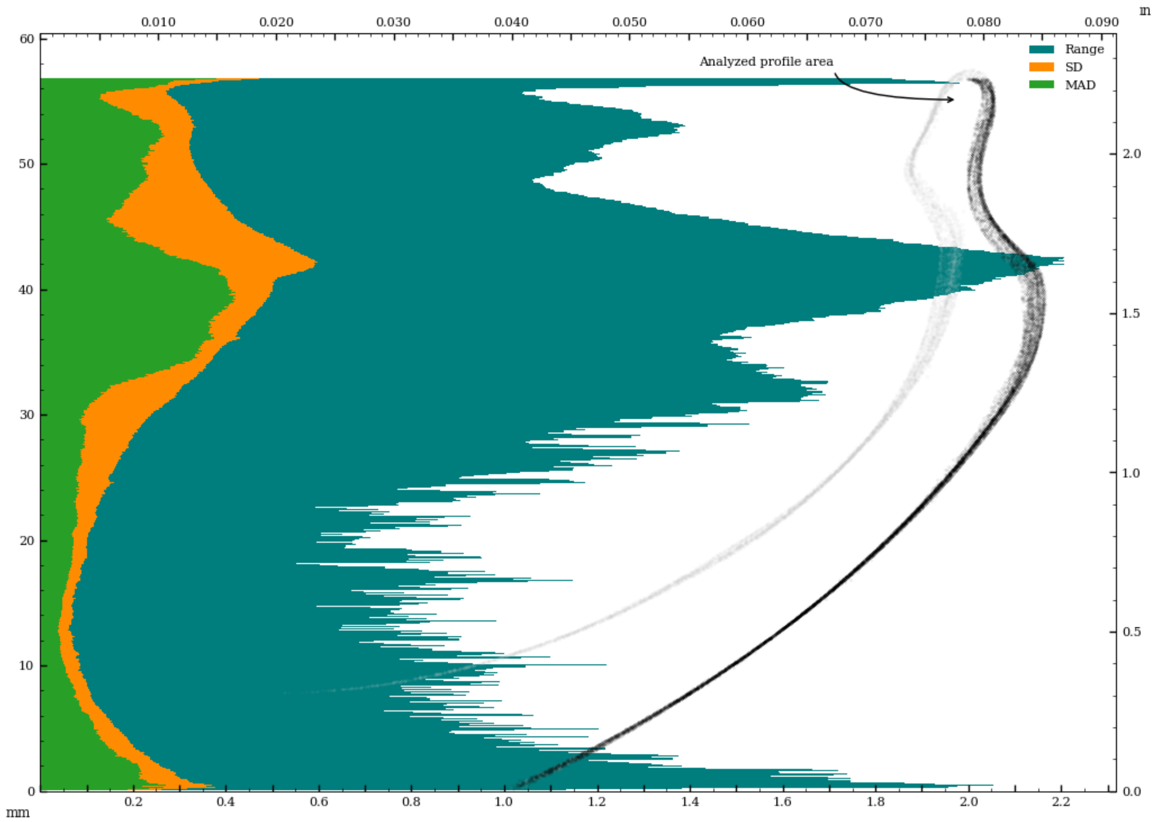

Figure 50: Circularity analysis of exterior surface - in z-plane

Circularity analysis of exterior samples perpendicular to surface curvature

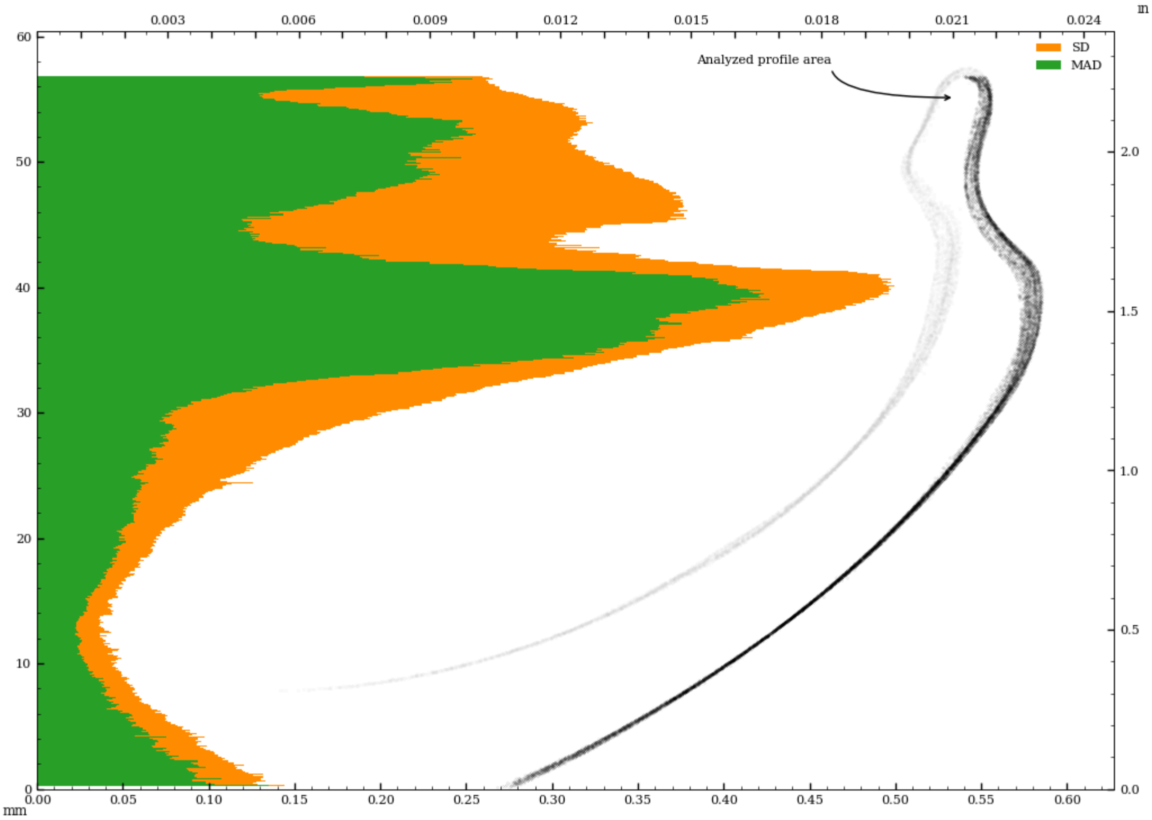

Figure 51: Circularity analysis of exterior samples perpendicular to surface curvature

Circularity analysis of exterior surface - in z-plane

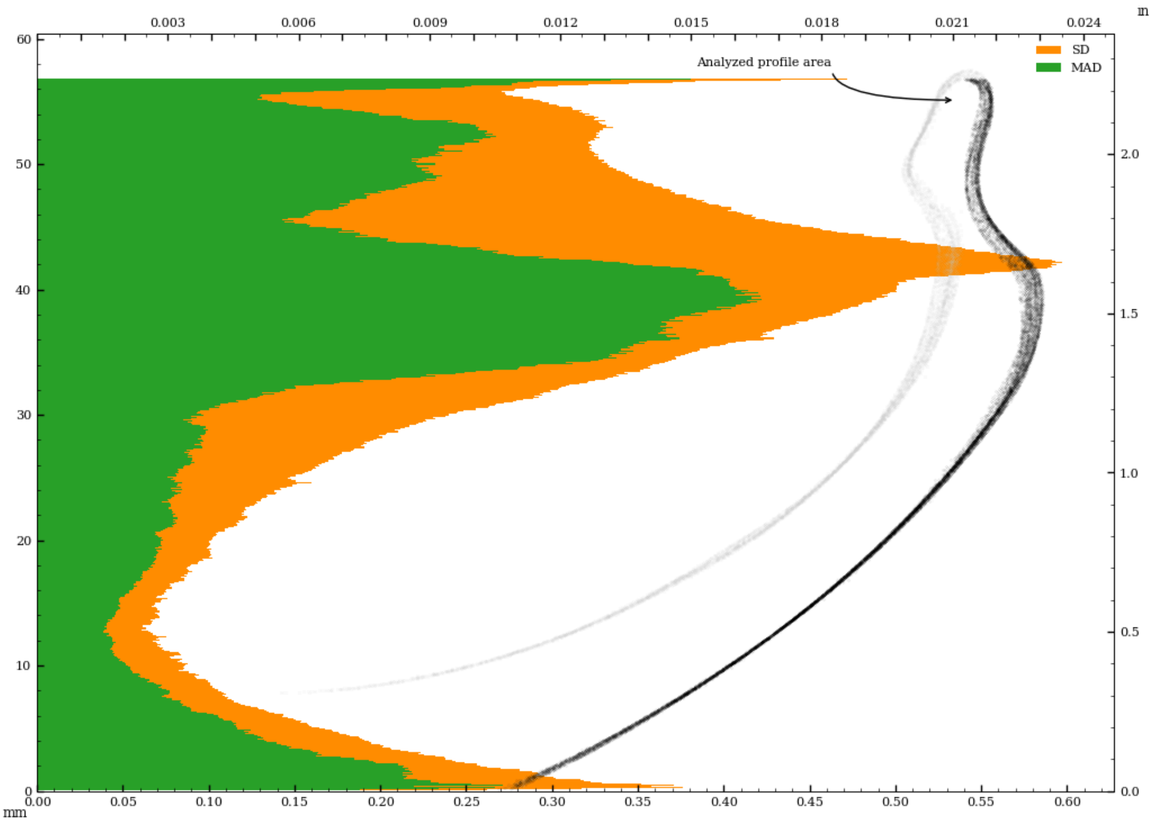

Figure 52: Circularity analysis of exterior surface - in z-plane

Circularity analysis of interior samples perpendicular to surface curvature

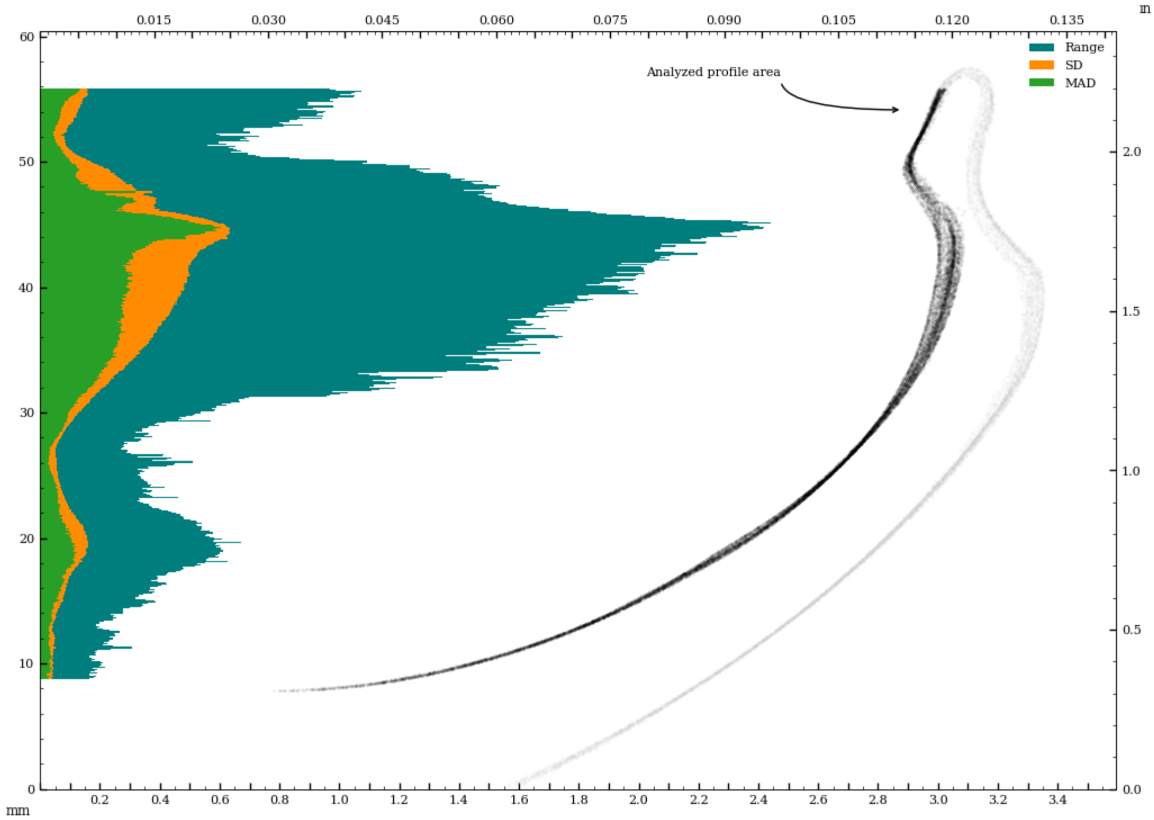

Figure 53: Circularity analysis of interior samples perpendicular to surface curvature

Circularity analysis of interior surface - in z-plane

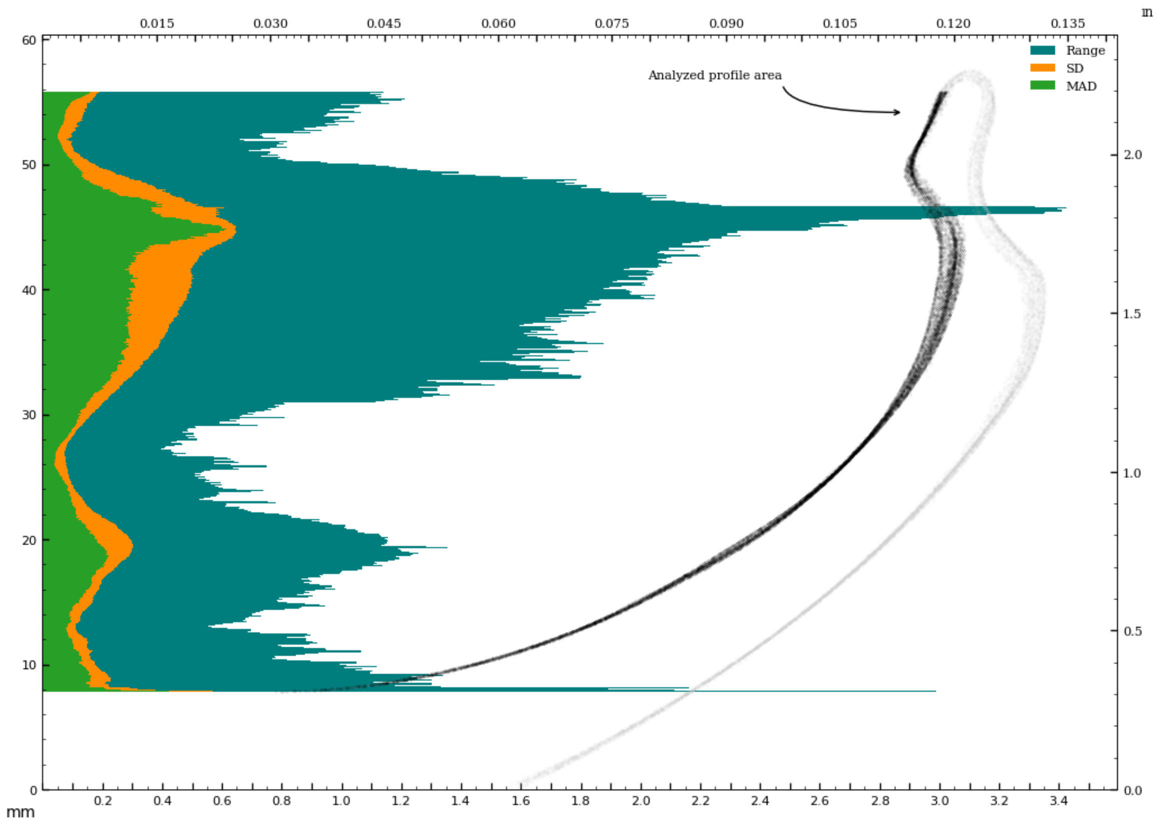

Figure 54: Circularity analysis of interior surface - in z-plane

Circularity analysis of interior samples perpendicular to surface curvature

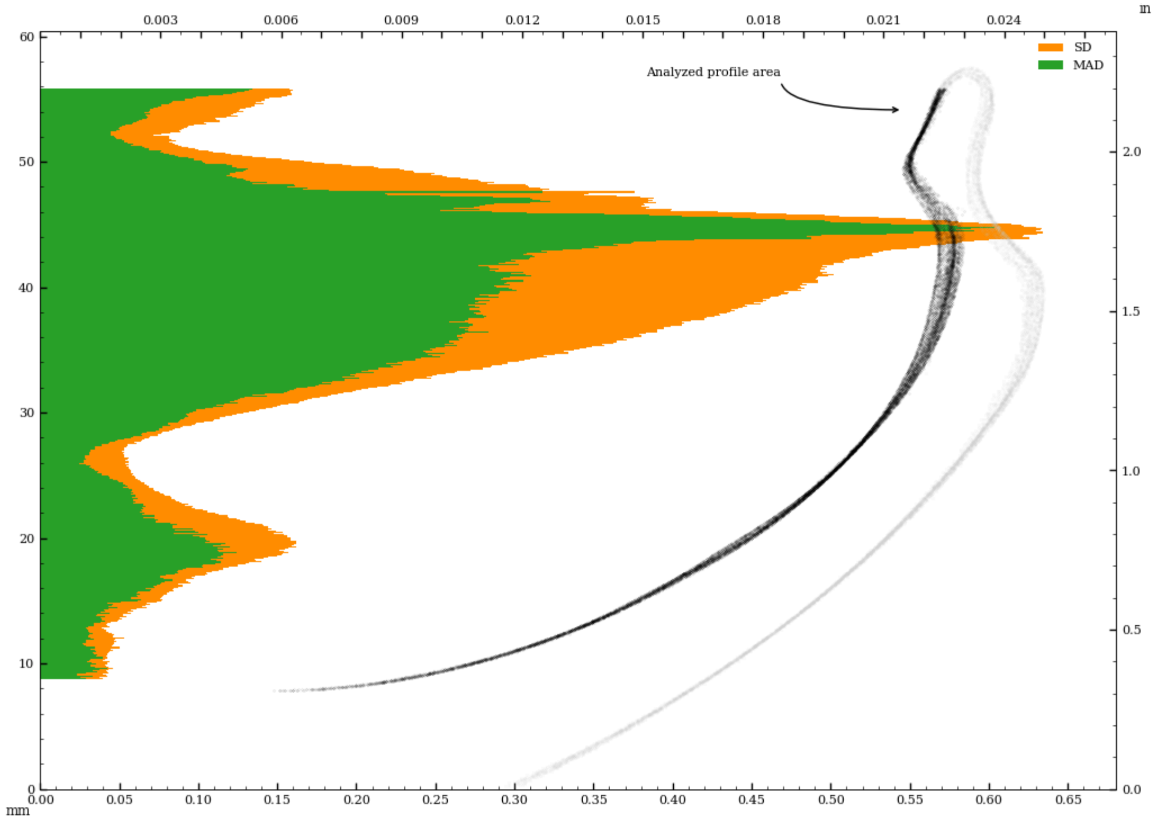

Figure 55: Circularity analysis of interior samples perpendicular to surface curvature

Circularity analysis of interior surface - in z-plane

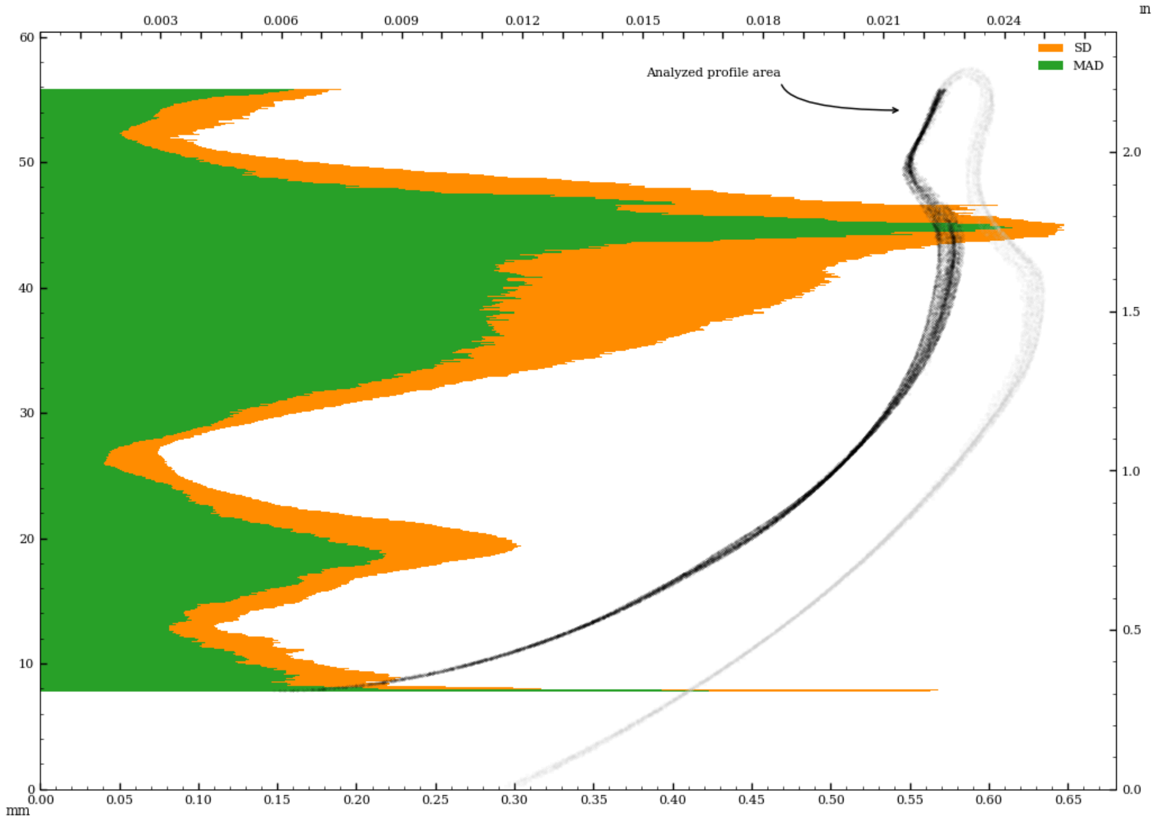

Figure 56: Circularity analysis of interior surface - in z-plane

Appendix B - Comparison Of Concentricity Measurements (Z-plane vs. surface-perpendicular)

Metric

Concentricity measurements perpendicular to surface curvature

Tag	Reference	Deviation	Sample size	Circle fit residuals analysis for sample listed in Tag column						
				Range full	**Range inliers**	**SD full**	**SD inliers**	**MAD full**	**MAD inliers**	**Center (x,y)**
		mm		mm	mm	mm	mm	mm	mm	µm
c01	z-axis	0.411	2726	1.175	1.175	0.310	0.310	0.218	0.218	−180, −369
c02	z-axis	0.186	3558	1.981	1.981	0.492	0.492	0.404	0.404	39, −182
c03	z-axis	0.141	2725	0.924	0.816	0.173	0.156	0.079	0.076	8, 141
c04	z-axis	0.042	1884	0.539	0.278	0.058	0.055	0.043	0.042	6, 41
c05	z-axis	0.016	1225	0.439	0.236	0.048	0.041	0.030	0.029	−3, −15
c06	z-axis	0.060	2404	0.557	0.313	0.081	0.070	0.058	0.057	−38, −47
c07	z-axis	0.622	4295	1.918	1.918	0.478	0.478	0.286	0.286	−620, −39
c08	z-axis	0.085	2218	0.384	0.384	0.093	0.093	0.078	0.078	−81, −27
c09	z-axis	0.032	943	0.499	0.499	0.123	0.123	0.102	0.102	27, 17
c10	z-axis	0.009	203	0.186	0.186	0.044	0.044	0.035	0.035	−9, −0
c01	c06	0.352	2726	1.175	1.175	0.310	0.310	0.218	0.218	−143, −322
c02	c07	0.675	3558	1.981	1.981	0.492	0.492	0.404	0.404	659, −143
c03	c08	0.190	2725	0.924	0.816	0.173	0.156	0.079	0.076	89, 168
c04	c09	0.033	1884	0.539	0.278	0.058	0.055	0.043	0.042	−21, 25
c05	c10	0.016	1225	0.439	0.236	0.048	0.041	0.030	0.029	6, −15

Concentricity measurements in z-plane

Tag	Reference	Deviation	Sample size	Circle fit residuals analysis for sample listed in Tag column						
				Range full	**Range inliers**	**SD full**	**SD inliers**	**MAD full**	**MAD inliers**	**Center (x,y)**
		mm		mm	mm	mm	mm	mm	mm	µm
c01	z-axis	0.445	2827	2.088	2.088	0.623	0.623	0.506	0.506	−200, −397
c02	z-axis	0.192	3528	2.190	2.190	0.562	0.562	0.392	0.392	40, −188
c03	z-axis	0.213	4091	1.618	1.450	0.363	0.338	0.266	0.259	8, 213
c04	z-axis	0.094	4233	0.757	0.629	0.158	0.157	0.132	0.131	10, 93
c05	z-axis	0.053	3988	0.997	0.626	0.114	0.110	0.072	0.071	−12, −52
c06	z-axis	0.078	3074	0.711	0.543	0.126	0.117	0.103	0.098	−47, −62
c07	z-axis	0.644	4504	1.994	1.994	0.526	0.526	0.333	0.333	−642, −48
c08	z-axis	0.145	3744	0.612	0.594	0.160	0.160	0.135	0.135	−138, −46
c09	z-axis	0.114	4156	1.194	1.194	0.272	0.272	0.185	0.185	96, 61
c10	z-axis	0.147	3525	1.067	1.067	0.200	0.200	0.153	0.153	−146, −20
c01	c06	0.369	2827	2.088	2.088	0.623	0.623	0.506	0.506	−153, −336
c02	c07	0.696	3528	2.190	2.190	0.562	0.562	0.392	0.392	681, −140
c03	c08	0.297	4091	1.618	1.450	0.363	0.338	0.266	0.259	146, 259
c04	c09	0.092	4233	0.757	0.629	0.158	0.157	0.132	0.131	−86, 32
c05	c10	0.138	3988	0.997	0.626	0.114	0.110	0.072	0.071	134, −32

Imperial

Concentricity measurements perpendicular to surface curvature

Tag	Reference	Deviation	Sample size	Circle fit residuals analysis for sample listed in Tag column						
				Range full	Range inliers	SD full	SD inliers	MAD full	MAD inliers	Center (x,y)
		in		in	in	in	in	in	in	thou
c01	z-axis	0.0162	2726	0.0463	0.0463	0.0122	0.0122	0.0086	0.0086	−7.1, −14.5
c02	z-axis	0.0073	3558	0.0780	0.0780	0.0194	0.0194	0.0159	0.0159	1.5, −7.2
c03	z-axis	0.0056	2725	0.0364	0.0321	0.0068	0.0061	0.0031	0.0030	0.3, 5.6
c04	z-axis	0.0016	1884	0.0212	0.0110	0.0023	0.0022	0.0017	0.0017	0.2, 1.6
c05	z-axis	0.0006	1225	0.0173	0.0093	0.0019	0.0016	0.0012	0.0012	−0.1, −0.6
c06	z-axis	0.0024	2404	0.0219	0.0123	0.0032	0.0028	0.0023	0.0022	−1.5, −1.8
c07	z-axis	0.0245	4295	0.0755	0.0755	0.0188	0.0188	0.0112	0.0112	−24.4, −1.5
c08	z-axis	0.0034	2218	0.0151	0.0151	0.0037	0.0037	0.0031	0.0031	−3.2, −1.0
c09	z-axis	0.0013	943	0.0196	0.0196	0.0048	0.0048	0.0040	0.0040	1.1, 0.7
c10	z-axis	0.0004	203	0.0073	0.0073	0.0017	0.0017	0.0014	0.0014	−0.4, −0.0
c01	c06	0.0139	2726	0.0463	0.0463	0.0122	0.0122	0.0086	0.0086	−5.6, −12.7
c02	c07	0.0266	3558	0.0780	0.0780	0.0194	0.0194	0.0159	0.0159	26.0, −5.6
c03	c08	0.0075	2725	0.0364	0.0321	0.0068	0.0061	0.0031	0.0030	3.5, 6.6
c04	c09	0.0013	1884	0.0212	0.0110	0.0023	0.0022	0.0017	0.0017	−0.8, 1.0
c05	c10	0.0006	1225	0.0173	0.0093	0.0019	0.0016	0.0012	0.0012	0.2, −0.6

Concentricity measurements in z-plane

Tag	Reference	Deviation	Sample size	Circle fit residuals analysis for sample listed in Tag column						
				Range full	Range inliers	SD full	SD inliers	MAD full	MAD inliers	Center (x,y)
		in		in	in	in	in	in	in	thou
c01	z-axis	0.0175	2827	0.0822	0.0822	0.0245	0.0245	0.0199	0.0199	−7.9, −15.6
c02	z-axis	0.0076	3528	0.0862	0.0862	0.0221	0.0221	0.0155	0.0155	1.6, −7.4
c03	z-axis	0.0084	4091	0.0637	0.0571	0.0143	0.0133	0.0105	0.0102	0.3, 8.4
c04	z-axis	0.0037	4233	0.0298	0.0248	0.0062	0.0062	0.0052	0.0052	0.4, 3.7
c05	z-axis	0.0021	3988	0.0392	0.0246	0.0045	0.0043	0.0028	0.0028	−0.5, −2.0
c06	z-axis	0.0031	3074	0.0280	0.0214	0.0050	0.0046	0.0041	0.0039	−1.9, −2.4
c07	z-axis	0.0253	4504	0.0785	0.0785	0.0207	0.0207	0.0131	0.0131	−25.3, −1.9
c08	z-axis	0.0057	3744	0.0241	0.0234	0.0063	0.0063	0.0053	0.0053	−5.4, −1.8
c09	z-axis	0.0045	4156	0.0470	0.0470	0.0107	0.0107	0.0073	0.0073	3.8, 2.4
c10	z-axis	0.0058	3525	0.0420	0.0420	0.0079	0.0079	0.0060	0.0060	−5.7, −0.8
c01	c06	0.0145	2827	0.0822	0.0822	0.0245	0.0245	0.0199	0.0199	−6.0, −13.2
c02	c07	0.0274	3528	0.0862	0.0862	0.0221	0.0221	0.0155	0.0155	26.8, −5.5
c03	c08	0.0117	4091	0.0637	0.0571	0.0143	0.0133	0.0105	0.0102	5.7, 10.2
c04	c09	0.0036	4233	0.0298	0.0248	0.0062	0.0062	0.0052	0.0052	−3.4, 1.3
c05	c10	0.0054	3988	0.0392	0.0246	0.0045	0.0043	0.0028	0.0028	5.3, −1.3